GEORGIA INSTITUTE OF TECHNOLOGY
OFFICE OF CONTRACT ADMINISTRATION
SPONSORED PROJECT INITIATION

Date: April 15, 1980

Project Title: The Effects of Powder Metallurgical Processing and Intermediate Thermal Mechanical Treatment on the Fatigue Properties of High Strength Aluminum Alloys

Project No: E-19-610

Co-Project Director: Dr. S.B. Chakrabortty and Dr. E. A. Starke, Jr.

Sponsor: U. S. Army Research Office; Research Triangle Park, N. Carolina 27709

Agreement Period: From April 1, 1980 Until March 31, 1983 (R&D Perf. Period

Type Agreement: Contract No. DAAG29-80-C-0100

Amount: $119,391 (Partially funded for $78,457 through 3/31/82)

Reports Required: Semi-annual Progress Reports; Final Technical Report

Sponsor Contact Person (s):

Technical Matters

Mr. George Mayer
Metallurgy and Materials Science
U. S. Army Research Office
P. O. Box 12211
Research Triangle Park, NC 27709

Contractual Matters
(thru OCA)

Mr. A. J. Van Hall (All Administrative no-funds actions)
Mr. H.T. Throckmorton (All funding actior
U. S. Army Research Office
P.O. Box 12211
Research Triangle Park, NC 27709

- - -

Mr. Thomas A. Bryant, ONR RR - Ga. Tech (Property Administration, Closing duties, etc.)

Defense Priority Rating: None

Assigned to: Chemical Engineering (School/~~Laboratory~~)

COPIES TO:

Project Director
Division Chief (EES)
School/Laboratory Director
Dean/Director—EES
Accounting Office
Procurement Office
Security Coordinator (OCA)
✓ Reports Coordinator (OCA)
Library, Technical Reports Section
EES Information Office
EES Reports & Procedures
Project File (OCA)
Project Code (GTRI)
Other C. E. Smith

GEORGIA INSTITUTE OF TECHNOLOGY OFFICE OF CONTRACT ADMINISTRATION

SPONSORED PROJECT TERMINATION/CLOSEOUT SHEET

Date March 27, 1984

Project No. E-19-610 School/~~Lab~~ ChE

Includes Subproject No.(s)

Project Director(s) Dr. S.B. Chakrabortty and Dr. E.A. Starke, Jr. GTRI / ~~GIT~~

Sponsor U.S. Army Research Office; Research Triangle Park, NC

Title The Effects of Powder Metallurgical Processing and Intermediate Thermal Mechanical Treatment on the Fatigue Properties of High Strength Aluminum Alloys

Effective Completion Date: 3/31/83 (Performance) 3/31/83 (Reports)

Grant/Contract Closeout Actions Remaining:

- [ ] None
- [x] Final Invoice or Final Fiscal Report DCAA
- [x] Closing Documents
- [x] Final Report of Inventions
- [x] Govt. Property Inventory & Related Certificate
- [ ] Classified Material Certificate
- [ ] Other

Continues Project No. Continued by Project No.

COPIES TO:

Project Director
Research Administrative Network
Research Property Management
Accounting
Procurement/EES Supply Services
Research Security Services
Reports Coordinator (OCA)
Legal Services

Library
GTRI
Research Communications (2)
Project File
Other

Form OCA 60:1028

PROGRESS REPORT

(TWENTY COPIES REQUIRED)

1. ARO PROPOSAL NUMBER: DRXRO-MS-17161

2. PERIOD COVERED BY REPORT: 4/1/80 - 12/31/81

3. TITLE OF PROPOSAL: The Effects of Powder Metallurgical Processing and Intermediate Thermal Mechanical Treatment on the Fatigue Properties of High Strength Aluminum Alloys.

4. CONTRACT OR GRANT NUMBER: ARO Contract No. DAAG29-80-C-0100

5. NAME OF INSTITUTION: Georgia Institute of Technology

6. AUTHOR(S) OF REPORT: Victor Kuo, S. B. Chakrabortty and E. A. Starke, Jr.

7. LIST OF MANUSCRIPTS SUBMITTED OR PUBLISHED UNDER ARO SPONSORSHIP DURING THIS PERIOD, INCLUDING JOURNAL REFERENCES:

NONE

8. SCIENTIFIC PERSONNEL SUPPORTED BY THIS PROJECT AND DEGREES AWARDED DURING THIS REPORTING PERIOD:

Victor Kuo (MS Student)
S. B. Chakrabortty
E. A. Starke, Jr.

Dr. S. B. Chakrabortty 17161-MS
Dr. E. A. Starke, Jr.
Georgia Institute of Technology
School of Chemical Engineering
Fracture and Fatigue Research Lab
Atlanta, GA 30332

BRIEF OUTLINE OF RESEARCH FINDINGS

Microstructure and texture of materials may be controlled to a large degree to obtain an improvement in a given mechanical property. This is usually achieved at the expense of another property. For example, one may get an improvement in fatigue stess-life or strain-life behavior by reducing the slip length through microstructural control. However, usually this also leads to a decrease in the resistance to fatigue crack growth. This research is directed towards understanding fatigue mechanisms in terms of microstructural variations produced by processing (i.e., ITMT and rapid solidification) and in optimizing microstructure to enhance fatigue initiation and crack growth resistance.

Four CT-91 alloys with different microstructures and textures were produced at Alcoa and provided by AMMRAAC for comparison of fatigue properties. Ingot alloys were conventionally processed (IMCP) or ITMT processed (IMIP). Powder alloys were conventionally processed (PMCP) or ITMT processed (PMIP-AR) and aged to the T7E70 condition. The microstructural analysis of IMCP showed a 30% degree of recrystallization, with large elongated pancake-shaped grains (grain size $\sim$ 3.5um) and a sharp texture. PMIP-AR was shown to have a 22% degree of recrystallization, with small grains ($\sim$ 4.5um) and a weak texture.

It is believed that the preferential oxidation of solute atoms (e.g., Mg) during air atomization caused the low yield strengths of powder alloys. Uniform deformation of small grains and the existence of a brittle oxide film on powder boundaries produces an intergranular fracture for the powder alloys. IMIP had low ductility caused by intense planar deformation of large grains and poor strain incompatibility across grain boundaries. The ingot alloys showed both intergranular and transgranular fracture.

Under strain-controlled fatigue tests, the best LCF properties were found for the small-grain powder alloys, which had short slip distances and uniform deformation, although there was a wide scatter band due to microstructural inhomogeneities (e.g., the distribution of oxides). For the ingot ITMT alloy, deformation concentrated in coarse slip bands, and since the slip distance was large, significant grain boundary slip offsets were produced. This resulted in the poorest properties. The fatigue cracks initiated at grain boundaries for powder alloys, while initiating at both grain boundaries and slip bands for ingot alloys.

In order to modify the grain structure, an extra cold-reduction was used on PMIP-AR alloy, followed by a recrystallization treatment, solution heat treatment and aging. Completely recrystallized microstructures with slightly flattened grains ($\sim$ 20um) and weak textures were obtained. For the T7E70 condition, this alloy (PMIP-GT) showed slightly improved LCF properties over those obtained previously for powder alloys. This may be attributed to the growth of recrystallized grains past the broken oxide film, and the difficulty of slip across high-angle grain boundaries.

All of the alloys were re-solution heat-treated, stretched ($\sim$ 1.5-2.0%) and peak-aged (T651) to make the grain boundary the major barrier for dislocation glide, thus enchancing the grain size and texture effects. In this condition, yield strengths and ductilities for the different materials are within 10%, with the exception of the poor ductility of the PMCP alloy. In a dry-air environment, the PMIP-GT alloy showed the best fatigue strain-life behavior. The PMCP alloy showed the worst strain-life behavior and a wide scatter band. The presence of shearable precipitates enhanced planar slip and low angle grain boundaries of the strongly textured PMCP alloy were not major barriers to slip. Consequently, this product behaved like a large-grain alloy, with poor ductility and poor LCF properties. The characteristics of a small-grain alloy were maintained, however, during FCP tests and the PMCP alloy had a faster crack growth rate and lower threshold ($\Delta K_{th} \sim 3.6$ MPa$\sqrt{m}$) than either the PMIP-GT ($\sim$ 4.1 MPa$\sqrt{m}$), IMIP ($\sim$ 4.8 MPa$\sqrt{m}$), or the IMCP ($\sim$ 4.8 MPa$\sqrt{m}$) alloys.

ITMT processing produces a more homogeneous microstructure and gives more uniform mechanical properties, especially for powder alloys. The powder ITMT processed alloy shows the best combination of fatigue crack initiation and propagation resistances.

PROGRESS REPORT

(TWENTY COPIES REQUIRED)

1. ARO PROPOSAL NUMBER: DRXRO-MS-17161

2. PERIOD COVERED BY REPORT: 1/1/81 - 6/30/81

3. TITLE OF PROPOSAL: The Effects of Powder Metallurgical Processing and Intermediate Thermal Mechanical Treatment on the Fatigue Properties of High Strength Aluminum Alloys.

4. CONTRACT OR GRANT NUMBER: ARO Contract No. DAAG29-80-C-0100

5. NAME OF INSTITUTION: Georgia Institute of Technology

6. AUTHOR(S) OF REPORT: Victor Kuo, S. B. Chakrabortty and E. A. Starke, Jr.

7. LIST OF MANUSCRIPTS SUBMITTED OR PUBLISHED UNDER ARO SPONSORSHIP DURING THIS PERIOD, INCLUDING JOURNAL REFERENCES:

NONE

8. SCIENTIFIC PERSONNEL SUPPORTED BY THIS PROJECT AND DEGREES AWARDED DURING THIS REPORTING PERIOD:

Victor Kuo (MS Student)
S. B. Chakrabortty
E. A. Starke, Jr.

Dr. S. B. Chakrabortty 17161-MS
Dr. E. A. Stake, Jr.
Georgia Institute of Technology
School of Chemical Engineering
Fracture and Fatigue Research Lab
Atlanta, GA 30332

BRIEF OUTLINE OF RESEARCH FINDINGS

The improvement of a given property through microstructural control is usually achieved at the expense of another property. The microstructural features which enhance the strength may not be good for ductility, and improvements in the resistances to fatigue crack initiation (FCI) and propagation (FCP) may be conflicting property goals. A reduction in grain size, for example, may improve the FCI resistance while sacrificing FCP resistance. However, it may be possible to optimize the microstructure by applying ITMT processing and powder metallurgical consolidation to obtain the best overall combination of fatigue properties and other mechanical properties.

The fatigue response to microstructural changes in the high strength aluminum alloy, CT91, will be systematically examined in this work. A wide variety of microstructures can be produced by using conventional processing (CP) and ITMT processing (IP) on both ingot metallurgical (I/M) and powder metallurgical (P/M) alloys. The major microstructural differences are due to changes in the grain parameters (e.g. grain size, grain shape, and texture) and the sizes and distribution of particles. The optimum microstructure for overall fatigue resistance, and correlations between fatigue properties and microstructural features, can then be determined.

Four CT91 alloys with different microstructures were developed by using either conventional processing (CP) or intermediate thermomechanical treatment (ITMT) on ingot-metallurgical (I/M) and powder-metallurgical (P/M) billets. Powder metallurgy produced a finer grain structure and particle distribution than ingot metallurgy. ITMT processing produced a recrystallized, coarse grain structure with a weak texture, compared to the unrecrystallized grain structure and sharp texture obtained with conventional processing. In order to study the effects of these microstructural features on mechanical properties, the cyclic and monotonic tests were conducted in the peak-aged condition, T651, in dry air. The low cycle fatigue (LCF) data were also collected in the overaged condition, T7E70.

Except for the conventionally processed P/M alloy, all materials had comparable monotonic properties. The resistance to fatigue crack initiation (FCI) increased with both a reduction in grain size and a finer particle distribution for both aging conditions. Smaller grain sizes and finer particle distributions reduced the degree of cyclic strain localization.

The conventionally processed P/M alloy had the poorest ductility and FCI resistance of the alloys in the T651 condition, although the slip was fairly homogeneous. This may be due to the presence of oxides at the grain boundaries and a lengthening of the slip distance due to a sharp texture. In the T7E70 condition, this alloy had a ductility similar to the other alloys, and the second best FCI resistance. Further homogenization of slip by the introduction of a large volume fraction of non-shearable precipitates, may reduce the effect of the sharp texture and delay the oxide-induced intergranular crack initiation.

The threshold stress intensity ranges, ΔK_{th}, and the fatigue crack growth rates (FCGR) roughly follow a grain size dependence. The resistance to fatigue crack propagation increases with increasing grain size. It appears that a large grain allows more reversible slip and reduces the amount of accumulated plastic strain within the reversed plastic zone.

The ITMT processing of CT91 powder produced an optimum microstructure: a fine, recrystallized, homogeneous grain structure with a fine particle distribution and weak texture. This resulted in the best overall mechanical properties including: comparable monotonic properties, superior fatigue crack initiation resistance and an intermediate fatigue crack growth rate.

PROGRESS REPORT

(TWENTY COPIES REQUIRED)

1. ARO PROPOSAL NUMBER: DRXRO-MS-17161

2. PERIOD COVERED BY REPORT: 7/1/81 - 12/31/81

3. TITLE OF PROPOSAL: The Effects of Powder Metallurgical Processing and Intermediate Thermal Mechanical Treatment on the Fatigue Properties of High Strength Aluminum Alloys

4. CONTRACT OR GRANT NUMBER: ARO Contract No. DAAG29-80-C-0100

5. NAME OF INSTITUTION: Georgia Institute of Technology

6. AUTHOR(S) OF REPORT: Victor Kuo, H. Chang, and E. A. Starke, Jr.

7. LIST OF MANUSCRIPTS SUBMITTED OR PUBLISHED UNDER ARO SPONSORSHIP DURING THIS PERIOD, INCLUDING JOURNAL REFERENCES:
Victor Wei-Chung Kuo, M.S. Thesis, Georgia Tech, August, 1981
"The Effects of Powder Metallurgical Processing and Intermediate Thermal Mechanical Treatment on the Fatigue Properties of High Strength Aluminum Alloys, X7091" (Manuscript in final stages of preparation for submission to scientific journal)

8. SCIENTIFIC PERSONNEL SUPPORTED BY THIS PROJECT AND DEGREES AWARDED DURING THIS REPORTING PERIOD:

Victor Kuo, M.S. Degree awarded August, 1981 (Currently PhD student)
H. Chang (MS Student)
S. B. Chakrabortty
E. A. Starke, Jr.

Dr. S. B. Chakrabortty 17161-MS
Dr. E. A. Stake, Jr.
Georgia Institute of Technology
School of Chemical Engineering
Fracture and Fatigue Research Lab
Atlanta, GA 30332

BRIEF OUTLINE OF RESEARCH FINDINGS

This research is directed toward understanding fatigue mechanisms in terms of microstructural variations produced by processing. Four primary processing methods are being used to vary the grain structure, crystallographic texture, and constituent phase and dispersoid particle size in the high strength aluminum alloy X7091. These include conventionally processed ingot metal, IMCP; conventionally processed powder metal, PMCP; ingot metal processed by intermediate thermomechanical treatments, IMIP; and powder metal processed by intermediate thermal mechanical treatments, PMIP. A major objective of this study will be to identify the microstructure that gives the optimum combination of fatigue crack initiation and fatigue crack propagation resistance.

Although the PMCP had the finest grain size, it had the lowest fatigue crack initiation (FCI) resistance. This is attributed to Al_2O_3 particles which are formed during atomization and segregate to grain boundaries during conventional processing. ITMT effectively moves the high angle grain boundaries away from the Al_2O_3 particles and the PMIP has the best combination of properties of the structure examined thus far. PMIP has a fine, recrystallized, homogeneous grain structure, a fine particle distribution and a weak texture; comparable monotonic properties to the other three structures, superior FCI resistance, and an intermediate fatigue crack growth rate.

The IMIP discussed in our last report had been ITMT processed at Alcoa using the procedure developed by Waldman et al[1] at Frankfort Arsenal. Unfortunately, this processing, which was originally developed for 7075 and 7050, produced a very large (~130 micron) recrystallized grain size. The large grain size enhanced strain localization effects and lowered the fatigue crack initiation resistance. We have reprocessed the I/M using an ITMT procedure similar to that described by Wert, Paton, Hamilton and Mahoney,[2] and obtained a 15 micron recrystallized grain size. The FCI resistance of this product was superior to both the IMCP and PMCP but somewhat inferior to the PMIP. The improvement in FCI resistance is associated with the finer grain structure. The failure to reach the FCI resistance of PMIP is due to the presence of large constituent phase particles formed during the slower solidification of the I/M product, and which act as FCI sites. Fatigue crack propagation studies are underway on the reprocessed I/M X7091.

Our initial study indicated that, in addition to the grain size, and particle size distribution, the texture may show a secondary effect on the fatigue properties

of X7091. In an alloy with a sharp texture, dislocations may shear through the slightly misoriented grain boundaries and continue on the parallel slip planes of neighboring grains. Therefore, the grain boundaries may no longer be the major slip barriers, and the slip length, an important parameter for both FCI and FCP resistance, may not be associated with the grain size. This phenomenom was reported earlier by Sanders and Starke[3] in their paper on the effect of ITMT on 7050 plate. However, variation in other microstructural parameters prevented their determining the significance of the texture effect. We are now attempting to clarify the effects of texture on X7091 plate. During the last six months we have developed procedures for developing both random and highly textured material with similar recrystallized grain size and precipitate structure. Measurements of the fatigue properties and mechanism studies will be conducted during the next report period.

References

1. J. Waldman, H. Sulinski, and H. Markus, Met. Trans. 5 (1974) p. 573.

2. J. A. Wert, N. E. Paton, C. H. Hamilton, and M. W. Mahoney, Met. Trans. 12A (1981) p. 1267.

3. R. E. Sanders, Jr. and E. A. Starke, Jr., Met. Trans. 9A (1978) p. 1087.

PROGRESS REPORT

(TWENTY COPIES REQUIRED)

1. ARO PROPOSAL NUMBER: DRXRO-MS-17161

2. PERIOD COVERED BY REPORT: 1/1/82 - 6/30/82

3. TITLE OF PROPOSAL: The Effects of Powder Metallurgical Processing and Intermediate Thermal Mechanical Treatment on the Fatigue Properties of High Strength Aluminum Alloys

4. CONTRACT OR GRANT NUMBER: DAAG29-80-C-0100

5. NAME OF INSTITUTION: Fracture and Fatigue Research Laboratory
Georgia Institute of Technology

6. AUTHOR(S) OF REPORT: Victor W. C. Kuo, H. Chang, and E. A. Starke, Jr.

7. LIST OF MANUSCRIPTS SUBMITTED OR PUBLISHED UNDER ARO SPONSORSHIP DURING THIS PERIOD, INCLUDING JOURNAL REFERENCES:

1. The Effects of ITMT's and P/M Processing on the Microstructure and Mechanical Properties of the X7091 Alloy

   presented at the Annual AIME meeting, Dallas, TX, February. 1982
   to be published in the Conference Proceedings and submitted to
   Metallurgical Transactions A for review.

8. SCIENTIFIC PERSONNEL SUPPORTED BY THIS PROJECT AND DEGREES AWARDED DURING THIS REPORTING PERIOD:

   Victor W. C. Kuo, Ph.D. student
   H. Chang, MS student
   E. A. Starke, Jr., Co-Principal Investigator

Dr. S. B. Chakrabortty 17161-MS
Dr. E. A. Stake, Jr.
Georgia Institute of Technology
School of Chemical Engineering
Fracture and Fatigue Research Lab
Atlanta, GA 30332

BRIEF OUTLINE OF RESEARCH FINDINGS

The results of this program were presented at the Annual AIME Meeting in Dallas, Texas, in February, 1982, and at the AROD P/M meeting in Charleston, South Carolina in June, 1982. A manuscript has been submitted for publication in Metallurgical Transactions A and is abstracted as follows:

The influence of microstructure and texture on the monotonic and cyclic properties of X7091-T651 was investigated. The various structures were developed from conventional ingot metallurgy (I/M), powder metallurgy (P/M) and intermediate thermal mechanical treatments (ITMT). P/M produced a finer grain structure and particle distribution than I/M. ITMT's produced a recrystallized, coarse grain structure with a weak texture, compared to the unrecrystallized grain structure and sharp texture obtained with conventional processing (CP).

All materials had comparable monotonic properties. The resistance to fatigue crack initiation (FCI) increased with both a reduction in grain size and a finer particle distribution. Smaller grain sizes and finer particle distributions reduced the degree of cyclic strain localization. The CP-P/M alloy had the poorest ductility and FCI resistance of all the materials, although the slip was fairly homogeneous. This may be due to the presence of oxides at the grain boundaries and a sharp texture. The threshold stress intensity, ΔK_{th}, and the fatigue crack growth rate (FCGR) roughly follow a grain size dependence with the resistance to fatigue crack propagation (FCP) increasing with increasing grain size. It appears that large grains allow more reversible slip and reduce the amount of accumulated plastic strain within the reverse plastic zone. It is also believed that a greater degree of fatigue crack closure, which may be associated with large grains and a rough FCP surface, results in a lower FCGR in the low ΔK region.

The ITMT of P/M X7091 produced the optimum microstructure giving the best combination of mechanical properties. The important features include a small recrystallized grain structure, a fine particle distribution, a weak texture, and a low concentration of oxides at grain boundaries.

Current Efforts

An ITMT process reported by Rockwell International Corporation was conducted on I/M X7091 aluminum alloy. This ITMT process produced a homogeneous, fully recrystallized grain structure with small grain size, a random texture and a modified particle distribution compared to those of the conventionally processed I/M X7091 Alloy.

Both conventionally processed and ITMT processed alloys have comparable monotonic properties. The ITMT processed alloy has an improved FCI resistance compared to that of the conventionally processed alloy since the FCI resistance increased with both a reduction in grain size and a finer particle distribution. Greater fatigue crack growth rate in ITMT material may be due to the small grain size. Coffin-Manson plot showed that the superiority of low cycle fatigue properties of ITMT alloy may be ranked in the second place among those alloys.

Neither of the above mechanical properties was as good as those of the ITMT P/M alloy, which may be accounted for by the existence of coarse intermetallic particles in the I/M alloy.

Work to date has shown that crystallographic texture can effect both FCI and FCP of X7091, and control of texture may lead to improvement in these properties. The recrystallization texture formation strongly depends on the conditions of metal working and annealing. Several different recrystallization textures or texture intensities will be introduced into a recrystallized X7091 plate, keeping other microstructural variables constant. The mechanical properties and their directionalities will be determined on these plates. The results will be correlated with the texture parameters, deformation behavior and fracture mode. The effects of recrystallization texture or texture intensity on the mechanical properties can then be clarified. The optimum microstructure with the best overall mechanical properties will also be defined for the X7091 P/M alloy.

GRAIN PARAMETERS

	$\bar{L}_a \times \bar{L}_t \times \bar{L}_s$ (μm^3)	D_{eq} (μm)	Ω_{max}	I_{max}/I_{random}
IMIP-R*	11.5x10.7x8.2	13.0	0.13	1.73
IMCP	170x61x20	61	0.76	18.04

MONOTONIC PROPERTIES

	Y.S. (MPa)	ELOG (%)	$\ln(A_0/A_f)$ (%)
IMIP-R	545	12.0	42
IMCP	549	15.9	40

Low Cycle Fatigue

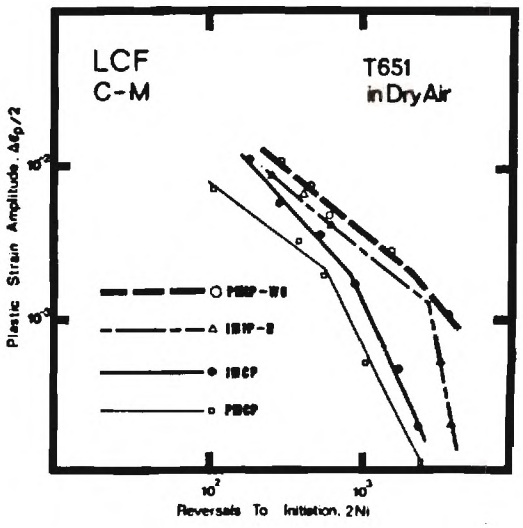

Fatigue Crack Propagation

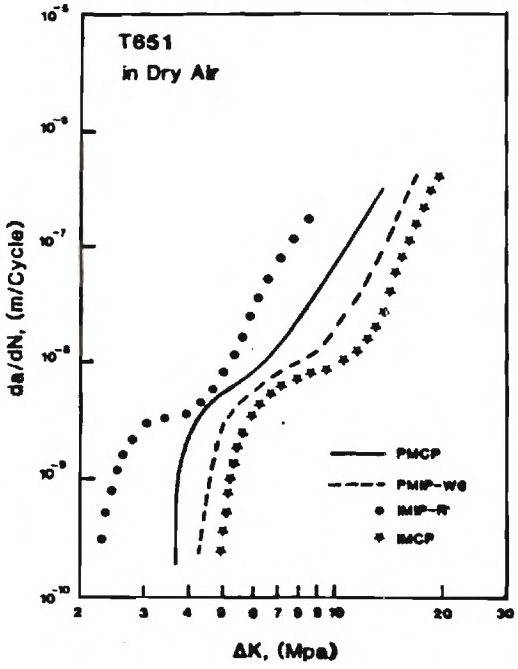

* IMIP-R: Rockwell ITMT

PROGRESS REPORT

(TWENTY COPIES REQUIRED)

1. ARO PROPOSAL NUMBER: 17161 MS

2. PERIOD COVERED BY REPORT: July 1, 1982 - December 31, 1983

3. TITLE OF PROPOSAL: The Effects of Powder Metallurgical Processing and Intermediate Thermal Mechanical Treatment on the Fatigue Properties of High Strength Aluminum Alloys

4. CONTRACT OR GRANT NUMBER: DAAG29-80-C-100

5. NAME OF INSTITUTION: Georgia Institute of Technology

6. AUTHOR(S) OF REPORT: Edgar A. Starke, Jr.

7. LIST OF MANUSCRIPTS SUBMITTED OR PUBLISHED UNDER ARO SPONSORSHIP DURING THIS PERIOD, INCLUDING JOURNAL REFERENCES:

Victor W. C. Kuo and E. A. Starke, Jr. "The Effect of ITMT's and P/M Processing on the Microstructure and Mechanical Properties of the X7091 Alloy" to appear in the March, 1983, issue of Metallurgical Transactions A.

8. SCIENTIFIC PERSONNEL SUPPORTED BY THIS PROJECT AND DEGREES AWARDED DURING THIS REPORTING PERIOD:

H. Chang (M.S. Student)
V. Kuo (Ph.D. Student)
E. A. Starke, Jr. Principal Investigator

Dr. S. B. Chakrabortty 17161-MS
Dr. E. A. Stake, Jr.
Georgia Institute of Technology
School of Chemical Engineering
Fracture and Fatigue Research Lab
Atlanta, GA 30332

BRIEF OUTLINE OF RESEARCH FINDINGS

A. Texture Effects in P/M

Our previous studies have indicated that the ITMT P/M alloy with small recrystallized grains, a fine particle distribution, and a weak texture has the best combination of mechanical properties, compared to other I/M and P/M X7091 alloys. It also suggested that, besides the grain size and particle distribution, crystallographic texture may have a secondary effect on the mechanical properties of these alloys. The current study is concerned with the clarification of texture effects on monotonic and cyclic properties. The optimum microstructure and texture for the best combination of mechanical properties can then be specified.

Several recrystallized P/M plates having a similar grain size ($\sim$ 25 μm), and particle distribution but different textures have been examined. These include a sharp retained deformation (SR) texture (maximum intensity/randomness, I_{max}/I_{rand}, = 5 to 9), a weak retained deformation (WR) texture (I_{max}/I_{rand} = 1.7 to 2.7), and a cube (C) texture (I_{max}/I_{rand} = 3 to 4). Properties of the SR plate were also measured 45 degrees to the rolling direction, SR-45. All these conditions showed similar monotonic properties in the T651 aging condition, with the exception of lower ductility for SR-45. SR-45 had a macroscopic shear fracture and microscopic mixed fracture mode which was in marked contrast to the cup-and-cone and transgranular fracture of the other conditions. This suggests that the SR orientation reduces the occurrence of multiple or homogeneous slip and increases the dislocation pile-up force on the grain boundaries. Laboratory air low and high cycle fatigue tests have been completed on the SR and WR plates. There were no obvious differences in either strain-life or stress-life plots. The aggressive laboratory air environment may overshadow the texture effect on fatigue crack initiation. However, the crack morphology of the SR specimens was relatively straight compared to the zigzag cracks of the WR specimen.

The fatigue crack growth rates (FCGR's) have been collected on the SR, SR-45, and C plates in vacuum. They showed similar threshold values ($\sim$ 5.5 MPa $m^{\frac{1}{2}}$) but a slight difference in the Paris region (FCGR:C > SR > SR-45). Crack branching, and a distinct valley-and-hill crack path were observed for SR and SR-45 plates, and saw-tooth crack path was observed for the C plate at low stress intensities. Even though different deformation structures and crack characteristics were present, there was no large effect of texture on the mechanical properties. This may be attributed to texture inhomogeneity through the thickness of the testing specimen. Further testing will be conducted in vacuum on thin sheet specimens which have a uniform texture through the thickness.

B. ITMT Ingot X7091

The present ITMT process produced a homogeneous, fully recrystallized grain structure with a 20 μm grain size, a modified particle distribution and random texture. Monotonic

and cyclic data have been collected in the peak-aged condition, T651, in dry air. The ITMT process has monotonic properties comparable to those previously reported (see attached preprint). However, the ITMT material has an improved fatigue crack initiation (FCI) resistance which may be due to its smaller grain size and finer particle distribution. The threshold stress intensity ΔK_{th}, and the fatigue crack growth rates (FCGR's) of all materials roughly follow a grain size dependence with FCGR decreasing with increasing grain size. The ITMT material generated in this research has the best FCI resistance and the poorest fatigue crack propagation (FCP) resistance among those I/M X7091 alloys. Its overall mechanical property combination is still inferior to that previously reported for the ITMT processed P/M X7091.

The Effect of ITMT's and P/M Processing on the Microstructure and Mechanical Properties of the X7091 Alloy

VICTOR W. C. KUO and E. A. STARKE, Jr.

The influence of microstructure and texture on the monotonic and cyclic properties of X7091-T651 was investigated. The various structures were developed from conventional ingot metallurgy (I/M), powder metallurgy (P/M) and intermediate thermal mechanical treatments (ITMT). Powder metallurgy produced a finer grain structure and particle distribution than I/M. Intermediate thermomechanical treatment produced a recrystallized, coarse grain structure with a weak texture, compared to the unrecrystallized grain structure and sharp texture obtained with conventional processing (CP). All materials had comparable monotonic properties. The resistance to fatigue crack initiation (FCI) increased with both a reduction in grain size and a finer particle distribution. Smaller grain sizes and finer particle distributions reduced the degree of cyclic strain localization. The CP-P/M alloy had the poorest ductility and FCI resistance of all the materials, although the slip was fairly homogeneous. This may be due to the presence of oxides at the grain boundaries and a sharp texture. The threshold stress intensity, ΔK_{th}, and the fatigue crack growth rate (FCGR) roughly follow a grain size dependence with the resistance of fatigue crack propagation (FCP) increasing with increasing grain size. It appears that large grains allow more reversible slip and reduce the amount of accumulated plastic strain within the reverse plastic zone. It is also believed that a greater degree of fatigue crack closure, which may be associated with large grains and a rough FCP surface, results in a lower FCGR in the low ΔK region. The intermediate thermomechanical treatment of P/M X7091 produced the optimum microstructure giving the best combination of mechanical properties. The important features include a small recrystallized grain structure, a fine particle distribution, a weak texture, and a low concentration of oxides at grain boundaries.

I. INTRODUCTION

HIGH strength Al-Zn-Mg-Cu (7XXX) alloys have been the subject of recent material application and development studies. The usage of conventionally processed 7XXX aluminum alloys is sometimes limited by low values of fatigue strength and fracture toughness. Improvements in some mechanical properties have been reported after modification of the microstructure by special processing techniques.[1-11] Microstructural modification studies have been conducted both with[9,10,11] and without[1-8] alloy compositional changes.

The important microstructural features of 7XXX aluminum alloys include the coherency and distribution of the age-hardening precipitates, the grain size, shape, and distribution, crystallographic texture, and the composition, structure size, shape, and distribution of the intermetallic particles. The effects of aging on mechanical properties have been widely investigated. Overaging tends to homogenize deformation improving fatigue crack initiation (FCI) resistance while decreasing the strength and fatigue crack propagation (FCP) resistance.[12-15] However, overaging may widen precipitate free zones (PFZ's) at grain boundaries, leading to poorer fracture properties if strain localization occurs within these regions.[16] A reduction in grain size usually promotes homogeneous deformation and reduces stress concentration at grain boundaries. This improves the ductility and FCI resistance,[5,6,17-19] but sometimes reduces the FCP resistance.[5,6,20,21] Large intermetallic particles tend to nucleate voids or cracks and small ones can promote void-sheet formation.[22,23] Introduction of a smaller volume fraction and/or a finer distribution of these particles results in an improved fracture toughness, FCI resistance, and FCP resistance in the high stress intensity range (ΔK).[4,23-28]

The effect of texture on the strength of materials as predicted by the Taylor relationship has been generally accepted.[29] Several recent reports[8,30,31] have described texture strengthening in some aluminum alloys. Sanders and Starke[5,6] reported that the sharpness of texture may have an important effect on the fracture and fatigue properties of 7050 and 7475 alloys. Slip incompatibility at grain boundaries of alloys having a random texture may lower fracture toughness and FCP resistance, when compared with sharply textured alloys. Simultaneously, the elimination of slip band decohesion as an FCI mechanism may enhance the FCI resistance for randomly textured alloys. However, the details of the texture effects on deformation and fracture are still not clear.

The precipitate structure can be controlled by aging treatments, and the other microstructural features can be controlled by primary processing procedures. Conventional hot-rolling of 7XXX alloys produces a coarse, inhomogeneous grain structure and intermetallic particle distribution which limits their mechanical properties. Intermediate thermomechanical treatments have been developed for obtaining a refined, recrystallized grain structure,[1-6] modified particle distribution,[3] and modified crystallographic textures.[5,6] The ITMT developed at Frankfort Arsenal[2] for 7XXX alloys involves the use of several high temperature

VICTOR W. C. KUO is Graduate Research Assistant, Fracture and Fatigue Research Laboratory, Georgia Institute of Technology, Atlanta, GA 30332. EDGAR A. STARKE, Jr., formerly Director, Fracture and Fatigue Research Laboratory, Georgia Institute of Technology, Atlanta, GA, is now Earnest Oglesby Professor of Materials Science, School of Engineering and Applied Science, University of Virginia, Charlottesville, VA 22901.

Manuscript submitted June 7, 1982.

treatments to precipitate Mg, Zn, and Cu as coarse particles. Warm working is then used to generate large dislocation densities at these particles. This provides a sufficient driving force for recrystallization to proceed during a subsequent anneal. The grain size of ITMT alloys is closely related to the number of coarse particles per unit volume.[32] The mechanical properties associated with the ITMT material include a strength similar to its CP counterpart, but improved ductility and lower fracture toughness values.[1-4] The resistance to FCI is slightly enhanced by ITMT's while the resistance to FCP is reduced.[5,6] Powder metallurgy processing produces alloys with fine, homogeneous grain structures and particle distributions. Comparisons of the mechanical properties of I/M and P/M 7075 extrusions (having the same composition) have shown that the P/M material had equivalent strength and ductility, but inferior fracture toughness. The P/M products, however, were more isotropic with respect to strength.[7,8] They also showed a better FCI resistance in the long-life range, but a greater FCGR at low ΔK.[8] Replacement of the dispersoid forming element Cr by Co or Fe + Ni resulted in higher monotonic and fatigue strengths and similar fracture toughness values, when compared to 7XXX I/M alloys.[9,10,11]

The improvement of a given property through microstructural control is usually achieved at the expense of another property. The microstructural features which enhance the strength may not be good for ductility, and improvements in the resistances to FCI and FCP may be conflicting property goals. A reduction in grain size, for example, may improve the FCI resistance while reducing FCP resistance. However, it may be possible to optimize the microstructure by applying P/M consolidation and ITMT's to obtain the best overall combination of fatigue and other mechanical properties. The effect of microstructural features produced by these processing methods on the monotonic and cyclic properties of the high strength aluminum alloy, X7091 (CT91), will be described in this paper.

II. EXPERIMENTAL

The materials used for this study consisted of plates produced by processing variations on an alloy with the same composition as the high strength aluminum, P/M alloy X7091 (Table I). The treatments included: conventionally processed I/M (IMCP), ITMT I/M (IMIP), conventionally processed P/M (PMCP), and ITMT P/M (PMIP). These alloys were prepared by the Alcoa Technical Center, Alcoa Center, Pennsylvania, using the processing schedules shown schematically in Figures 1(a) and 1(b). The ITMT's of Figure 1(b) were essentially the same as the FA-ITMT schedule reported for I/M 7075 as-recrystallized + hot-rolled (AR + HR).[2] The materials were received as 25.4 mm thick plates in the T7E70 overaged condition (Table II). Metallographic examination of the as-received PMIP plate revealed a partially recrystallized grain structure, which was not desired for this program. The PMIP plate was re-processed using the ITMT shown schematically in Figure 1(c). All of the alloying elements were first precipitated as coarse particles. The plate was then subjected to a warm (408 K) reduction of 50 pct by cross-rolling, followed by a recrystallization treatment to obtain the as-recrystallized (AR) condition.

In order to assess the effect of microstructure on the mechanical properties of an age-hardening alloy, it is convenient to choose an aging condition for which the effects of the various microstructural parameters are most pronounced. In the peak-aged temper, dislocations shear the

Table I. Chemical Composition of the X7091 Billets

Product Form	Composition in Wt Pct				
	Al	Zn	Mg	Cu	Co
Ingot	Bal.	6.33	2.33	1.54	0.43
Powder	Bal.	6.00	2.27	1.51	0.42

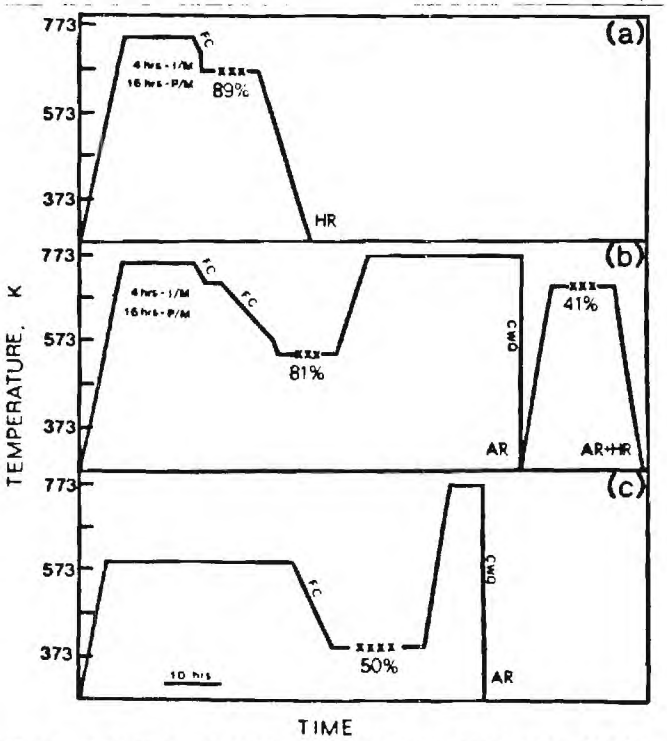

Fig. 1 — Processing schedules of (*a*) conventional processing, (*b*) FA-ITMT AR + HR processing, and (*c*) additional ITMT AR processing on the as-received PMIP alloy.

Table II. Aging Treatments for the X7091 Plates

T7E70	T651
Solution heat treat @ 761 ±5.6 K for 1 hour	Solution heat treat @ 761 ±5.6 K for 1 hour
Cold water quench	Cold water quench
Age at room temperature, 4 days minimum	Stretch 1.5 to 2.0 pct
Artificial age 24 hours @ 394 ±5.6 K	Age at room temperature, 4 days minimum
Second step age 14 hours @ 436 ±5.6 K	Artificial age 24 hours @ 394 ±5.6 K

coherent and partially-coherent strengthening precipitates.[12] Consequently, the deformation mode is predominately planar,[13] and both grain boundaries and intermetallic particles can serve as barriers to slip. The reprocessed PMIP plate and the rest of the as-received plates were re-solution heat treated, cold water quenched, stretched 1.5 to 2.0 pct, and aged to the peak-aged condition, designated T651 in Table II.

Optical metallographic samples were taken from the three principal orthogonal planes. Keller's reagent was used for the I/M alloys, and an etchant consisting of 84 ml H_2O, 15.5 ml HNO_3, 0.5 ml HF, and 3 g CrO_3[21] was used for the P/M alloys. Transmission electron microscopy (TEM) and scanning electron microscopy (SEM) were used to analyze intermetallic particle distributions and microstructural details. Foils for TEM were electropolished in a 1:2 HNO_3:methanol solution at 253 K. SEM specimens were etched in a 1:9 bromine:methanol solution at its boiling point. Quantitative microstructural parameters were determined by the mean intercept length and point count methods.[33]

Crystallographic texture determinations were carried out using the reflection method. Fixed time increments were employed to collect intensity data over a polar orientation range from 0 to 70 degrees. A computer program was used to construct the pole figures in the form of equal value contours and provided average, maximum, and minimum intensities.

All mechanical tests were performed on a closed loop servohydraulic machine. The specimens were taken from the central portions of the plates with the stress axes parallel to the rolling (longitudinal) direction. The cylindrical specimens had a diameter of about 4.8 mm and a gage length of 22 mm for the tension tests and 10.2 mm for the low cycle fatigue (LCF) tests. They were mechanically polished through 1 μm diamond paste. The tension-compression LCF tests ($R = -1$) were conducted in dry air ($R.H. < 0.2$ pct) using a strain rate of $10^{-3}s^{-1}$. An axial extensometer was attached to the specimen to control the total strain range, $\Delta\varepsilon_T$. The plastic strain range, $\Delta\varepsilon_p$, was determined from the width of the monitored hysteresis loop. The failure criterion was the number of reversals to macroscopic crack growth, $2N_f$, which we associated with a tensile load drop of 2 pct from the saturation level. However, the exact cycle at which the initiation of the fatal crack(s) occurs is somewhat ambiguous using macroscopic measurements.

Crack propagation tests were conducted in dry air using WOL-type compact-tension specimens ($H/W = 0.97$, thickness = 7.1 mm), an R ratio of 0.1, and a frequency of 10 Hz. The crack propagated in the long-transverse direction on a plane normal to the rolling direction. The crack length, a, was measured with a traveling microscope. During precracking near the threshold level, the load range was reduced 10 pct whenever the crack advanced out of the previous plastic zone. ΔK_{th} was determined from the load range at which the crack grew less than 0.1 mm during 10^6 cycles. The FCP data were taken for every 0.25 mm of growth for a/W's from 0.3 to 0.7. The load range was raised 5 pct after each reading, and then held constant as the FCP entered the Paris region of the FCGR curve.

SEM was used to examine the fracture features. Thin foils selected from the gage sections of the fractured LCF specimens were prepared to study the deformation behavior by TEM.

III. RESULTS AND DISCUSSION

A. *Microstructure*

The basic microstructural data obtained from optical microscopy are summarized in Table III. Conventional processing of the I/M produced a partially recrystallized microstructure with large, elongated, pancake-shaped grains (Figure 2(a)). The grain size of the IMCP alloy was measured between the easily distinguished, high-angle grain boundaries. The diameter of a sphere of equivalent volume as the irregularly shaped grain, D_{eq}, was 81 μm. The ITMT of the I/M produced a completely recrystallized microstructure with coarse, irregularly shaped grains, $D_{eq} = 130$ μm

Table III. Basic Microstructural Data of the X7091 Materials

Material	$\bar{L}_{\parallel} \times \bar{L}_{\mid} \times \bar{L}_{\perp}$ $(\mu m)^3$	$D_{eq}(\mu m)$	$\Omega_{pl\text{-}lin}$	DR (Pct)
IMCP	170 × 61 × 20	81	0.76	20 to 40
IMIP	139 × 109 × 76	130	0.33	100
PMCP	3.2 × 3.4 × 2	3.5	0.22	7
PMIP(AR)	4.1 × 5 × 2.4	4.5	0.24	22
PMIP	31.2 × 30.4 × 9.6	25.9	0.53	100

$\bar{L}$ = mean grain intercept length
$\parallel$ = longitudinal direction
$\mid$ = long-transverse direction
$\perp$ = short-transverse direction
D_{eq} = diameter of a sphere of equivalent volume
$\Omega_{pl\text{-}lin}$ = orientation factor of grain shape (*e.g.*, 0 for a sphere, 1 for a sheet)[33]
DR = degree of recrystallization

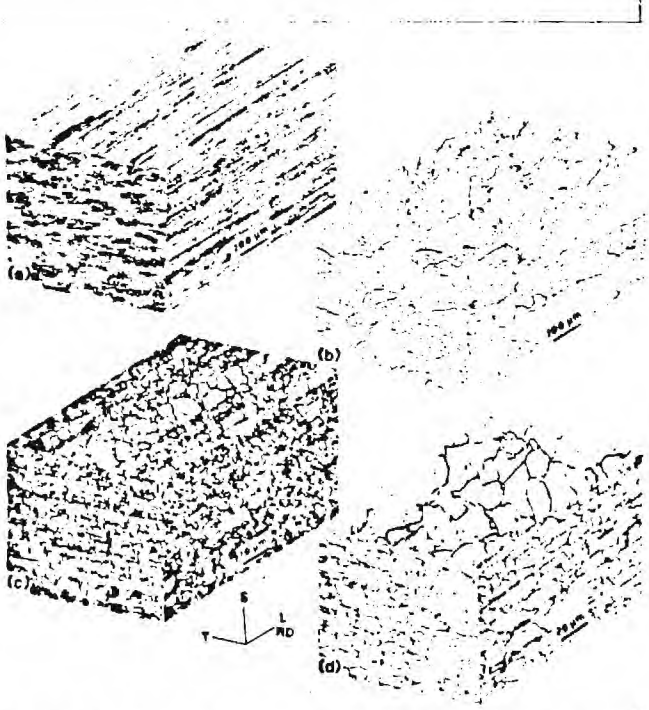

Fig. 2—Optical metallographs: (*a*) IMCP, (*b*) IMIP, (*c*) PMCP, and (*d*) PMIP.

(Figure 2(b)). Particles larger than 0.1 μm were observed on the bromine-etched surfaces by SEM. The particles in the IMCP material were in the form of coarse stringers aligned in the longitudinal direction with a spacing in the transverse direction of about 50 μm, (Figure 3(a)). The ITMT produced a more uniform distribution of particles in the IMIP material (Figure 3(b)). The particle sizes in these I/M's ranged from 0.1 μm to 15 μm. Energy dispersive X-ray analysis (EDXA) was used to demonstrate the presence of two types of particles (constituent phases) in the I/M's: cobalt-rich and copper-rich, which cannot be distinguished by shape or size. These particles were further identified as Al_9Co_2, Al_7Cu_2Fe, and Al_2CuMg from electron diffraction patterns. The presence of Al_2CuMg phase in the I/M 7XXX alloys has been discussed by Sanders and Starke.[5,6] The total volume fractions of particles observable by SEM were estimated by a point count method, and are listed in Table IV. The I/M materials had a slightly higher volume fraction of particles when compared with the P/M materials, and the CP materials had a higher volume fraction than those processed by ITMT. The substructure and recrystallized structure of the I/M materials are illustrated in Figures 4(a) and 4(b).

Previous studies[1-3,5,6] have shown that ITMT's produce a finer grain structure than CP for 7050, 7075, and 7475 I/M alloys. The ITMT method used in this study, with essentially the same processing schedule, developed a coarser grain structure for the I/M material. Nes[34] has indicated

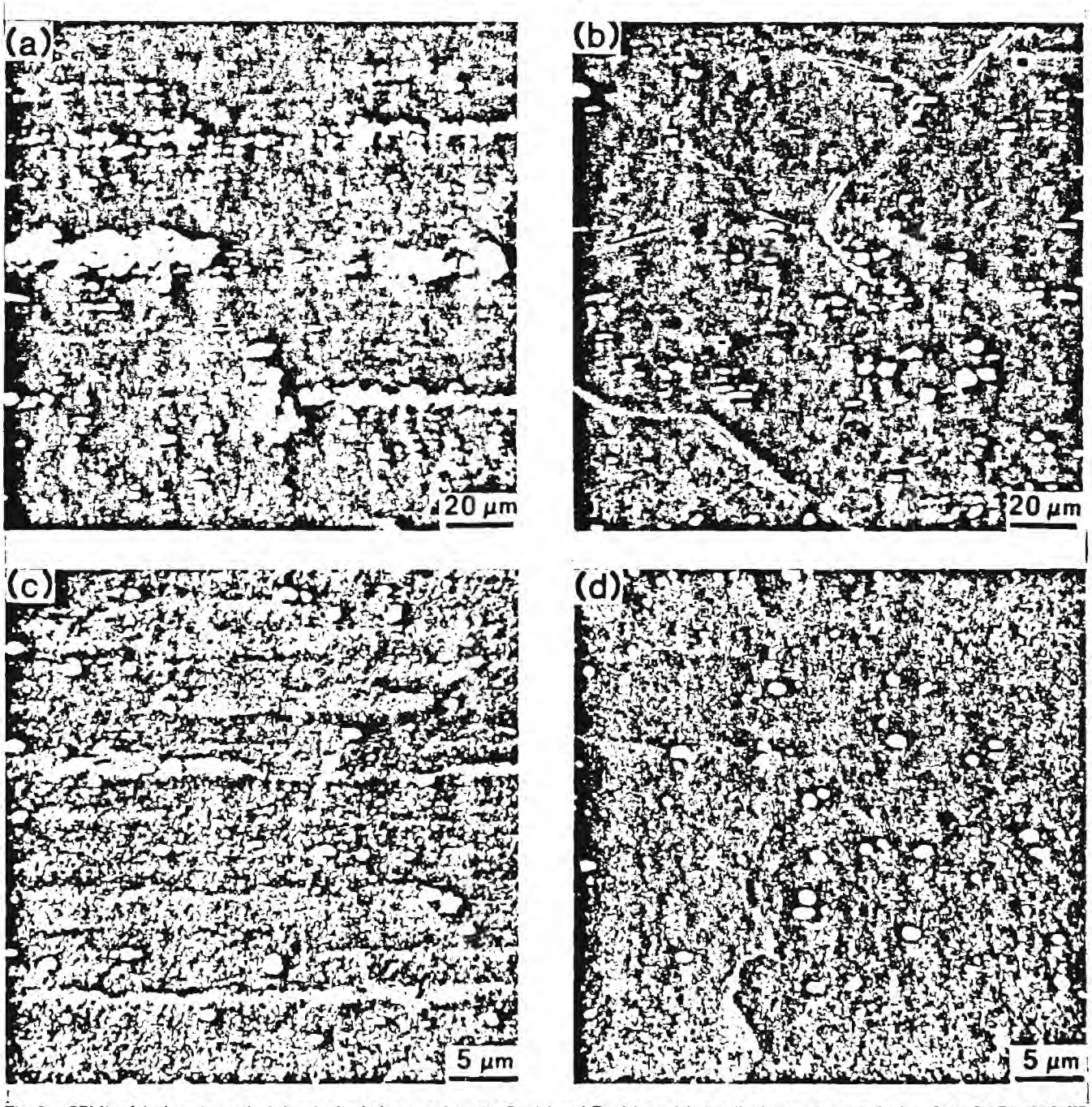

Fig. 3 — SEM's of the bromine-etched, longitudinal planes to show the Co-rich and Cu-rich particle distributions and morphologies of: (*a*) IMCP, (*b*) IMIP, (*c*) PMCP, and (*d*) PMIP.

Table IV. Total Volume Fraction of the Al_9Co_2 and Cu-Rich Particles with Sizes Larger Than 0.1 μm in the X7091 Materials

	Volume Fraction in Pct			
	IMCP	IMIP	PMCP	PMIP
Transverse plane	2.17	2.23	1.55	1.52
Longitudinal plane	2.56	1.98	1.74	1.71
Rolling plane	2.36	2.12	1.52	1.42
Average	2.36	2.11	1.60	1.55

that, in commercial aluminum alloys, the particles having sizes larger than 0.5 to 1.0 μm serve as heterogeneous recrystallization sites, and the presence of small particle dispersions retard nucleation. Therefore, the grain structures of ITMT materials should be closely related to their particle distribution during fabrication. The coarse particles and overaged precipitates prior to the medium temperature rolling act as recrystallization sites,[32] and the small dispersoids hinder recrystallization and grain growth.[5,6] A finer grain structure than for CP results for other ITMT I/M alloys. The coarser grain structure of IMIP may be attributed to the nonoptimum overaged precipitate structure of this ITMT schedule producing an insufficient number of nucleation sites. Wert *et al*[32] have recently correlated the particle size and number density with the recrystallized grain size of ITMT-7075.

Conventional processing produced an unrecrystallized microstructure with fine polygonized subgrains in the P/M alloy (Figure 2(c)). The grain size (3.5 μm) of the PMCP material was determined by considering either a recrystallized grain or a subgrain as one grain. The FA-ITMT AR + HR schedule for the P/M resulted in only a 22 pct degree of recrystallization (DR). This also suggests that the FA-ITMT schedule does not provide an optimum overaged precipitate structure for recrystallization nucleation. Further processing of PMIP plate produced a completely recrystallized microstructure of pancake-shaped grains having a low aspect ratio (Figure 2(d)). The final grain size, D_{eq} = 25 μm, which is larger than PMCP's, may be associated with the number of nucleation sites available for recrystallization.[32]

A finer, more random particle distribution existed in the rapidly solidified P/M than in the I/M, and both P/M materials showed similar particle distributions, regardless of processing (Figures 3(c) and 3(d)). The particle size of the powder alloys ranged from 0.1 μm and 2 μm. Most of the particles were spherical in shape. Particles of Al_9Co_2 and Al_7Cu_2Fe were identified by electron diffraction, and the Al_9Co_2 occurred more frequently. The low volume fraction of Al_7Cu_2Fe may be due to iron entering the Al_9Co_2, as observed by other workers.[35] No Al_2CuMg was found. Smaller particle volume fractions were observed in the P/M materials by SEM (Table IV) compared with the I/M counterparts. The theoretical volume fraction of Co particles, 1.16 pct, was calculated for both I/M and P/M materials, assuming a cobalt solubility of ~0.2 pct at 930 K.[10] The remaining particle volume fraction should consist of Cu-rich particles. This indicates a smaller amount of coarse Cu-rich particles was precipitated in the P/M materials, as expected when considering the difference in solidification rates between I/M and P/M products.

The oxides were seldom observed with the bromine-etch technique. TEM showed that the oxides were usually located at grain boundaries of the PMCP in the form of stringers (Figure 4(c)). The high angle boundaries appeared to correspond to the original powder particle boundaries; however, the particles were flattened into a pancake shape by rolling to a thickness of about 2 μm. The ITMT broke up the oxide stringers and moved the recrystallized grain boundaries away from the oxide particles. The modified homogenization schedule recrystallized the grain structure into a coarser size than that of CP P/M material.

The pole figures (Figure 5) were generated from X-ray diffraction intensities of {111} planes. In addition to the orientation distribution, quantitative information is printed below the pole figure. These numbers represent, in descending order, the average intensity in the area over which the X-ray data were collected, the maximum intensity divided by the average intensity, and the minimum intensity divided by the average intensity. The sharpness of a certain type of texture can be quantified by using these numbers. The maximum value also indicates the probability of misorientation across grain boundaries. Partially recrystallized IMCP and unrecrystallized PMCP (Figures 5(a) and 5(c)) both showed strong {358}⟨835⟩ textures with weak {110}⟨112⟩ textures. Previous investigators[36,37,38] referred to this type of annealing texture as a retained deformation texture, developed by polygonization.[38] The IMIP alloy had a random texture (Figure 5(b)), and the recrystallized, cross-rolled PMIP a weak {110}⟨112⟩ texture (Figure 5(d)).

B. *Monotonic Properties*

The monotonic properties obtained from the tensile tests are listed in Table V. All of the materials had similar yield strengths with the lowest value being for the PMIP. There is no direct relationship between the yield strength and the grain size for these materials in the peak-aged condition. The high strengthening effect associated with age hardening dominates all other contributions, *e.g.*, those due to grain size and texture.[2,5,6] Yield strengths lower than that of CP have been reported for ITMT 7475[5] and 7075[2] alloys. The nonuniform distribution of solute elements due to a short homogenization time after extensive overaging may be responsible for the slightly lower yield strengths of the ITMT-AR alloys. The ductilities of these materials, with the exception of PMCP, were similar and comparable to those of other 7XXX I/M alloys.[1,2,5,6] The ductility of PMCP was lower by about 30 pct.

A study of the deformation mode showed that slip was mostly planar (Figure 6), due to the dominance of a dislocation shearing mechanism in the peak-aged condition.[12,13] Localized deformation in the narrow PFZ's along the grain boundaries was not observed. The PFZ's may not be an important parameter for the monotonic deformation of these alloys.Other studies indicated that a reduction in grain size[19,39,40] or the presence of small incoherent particles[25,26] promotes homogeneity, and these factors may contribute to the observed improvement in ductility. However, the small grain size does not have this beneficial effect on the PMCP material. Figure 6(b) shows that the dislocation pile-ups may overcome the slightly misoriented grain boundaries in the materials having a sharp texture. Deformation may continue on nearly parallel slip systems in adjacent grains, thus

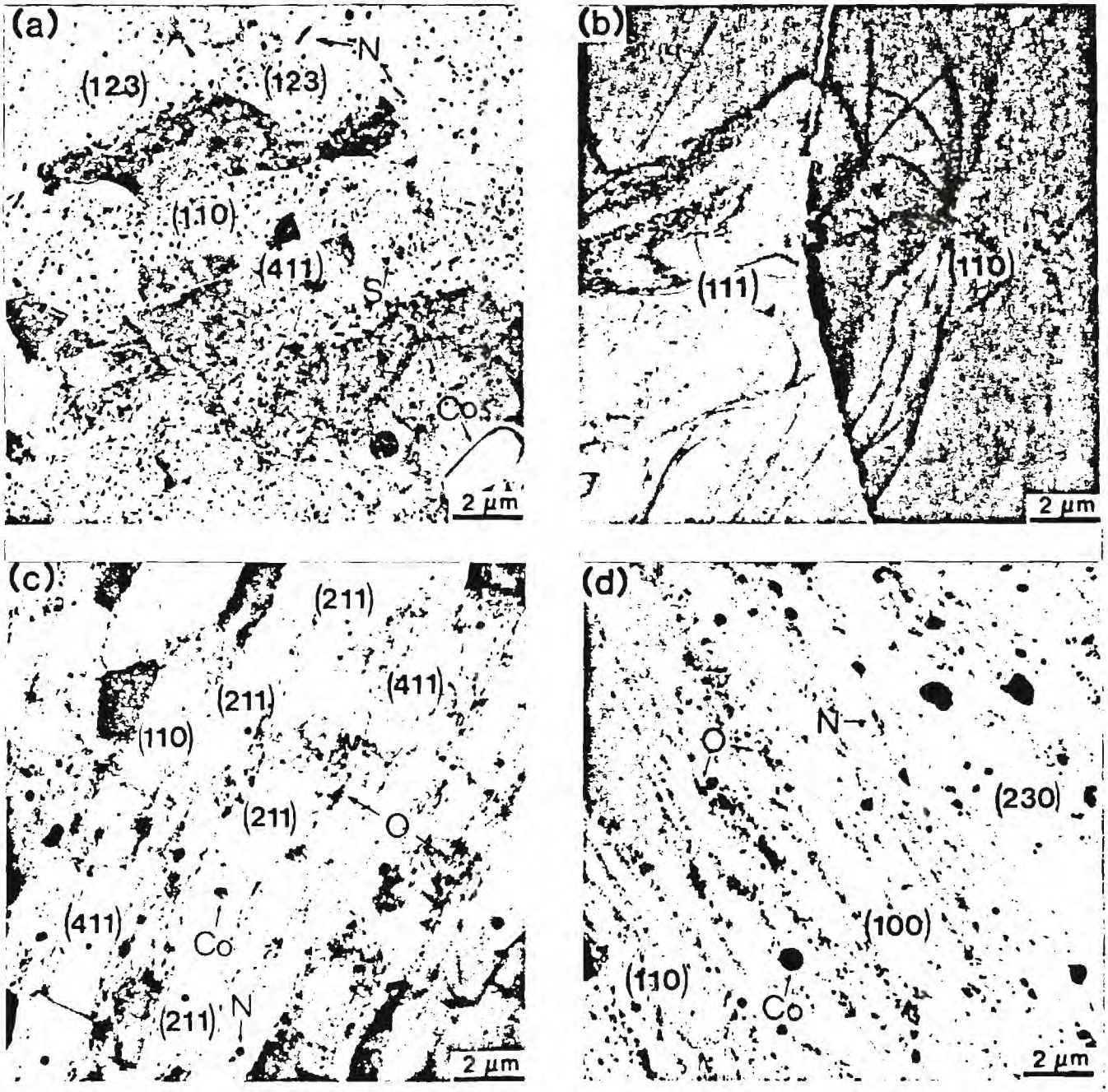

Fig. 4—TEM's of transverse planes of the as-received or as-reprocessed experimental materials in the T7E70 condition: (*a*) IMCP, (*b*) IMIP, (*c*) PMCP, and (*d*) PMIP. (Co: Al_9Co_2, N: Al_7Cu_2Fe, S: Al_2CuMg, O: oxides).

eliminating grain boundaries as effective barriers to slip, and possibly increasing the slip length. This mechanism would normally enhance transgranular shear fracture, and this was observed for the IMCP material (Figure 7(a)). However, the low ductility, highly textured PMCP material failed intergranularly (Figure 7(c)). The fracture features appeared as pulled-out flat grains, corresponding to the shape of the flattened powder particles and indicating fracture along the particulate boundaries which had a high oxide concentration.

For the materials with weak textures, multiple slip occurred to accommodate grain boundary incompatibility during deformation,[39,40,41] increasing the homogeneity of deformation. This effect and the uniform particle distribution of the IMIP materials compensated for the adverse effect of a large grain size and contributed to a ductility comparable to that of the IMCP material. The intergranular component of the fracture (Figure 7(b)) was probably associated with a long dislocation pile-up length[19] and a weak texture. The ITMT of the P/M material changed the fracture mode from intergranular for the PMCP to a mixed mode for the PMIP (Figure 7 (d)). The recrystallization process associated with the ITMT dissociated the grain boundaries from the oxides and reduced the occurrence of

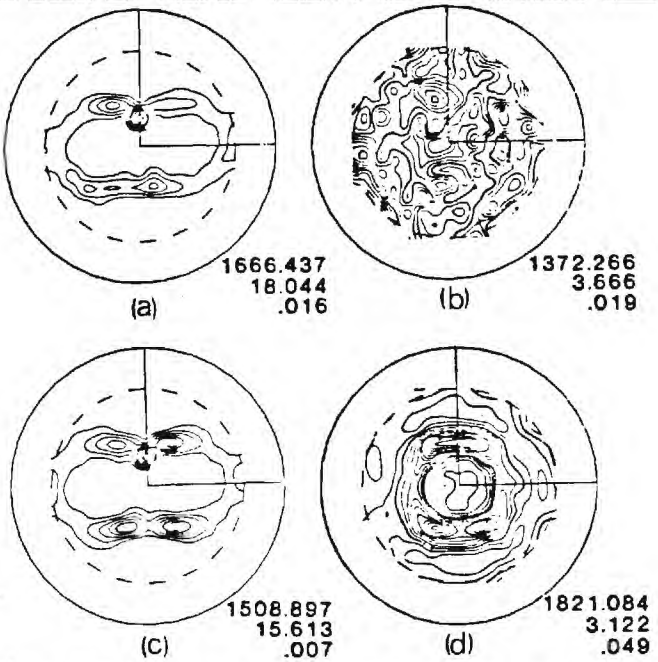

Fig. 5—{111} pole figures of the (*a*) IMCP, (*b*) IMIP, (*c*) PMCP, and (*d*) PMIP. (First number: randomness, second number: maximum intensity, third number: minimum intensity.)

intergranular fracture. The PMIP material had a ductility comparable to those of 7XXX I/M alloys[1,2,5,6] and higher than those of 7XXX P/M alloys.[8-11]

C. *Fatigue Deformation and Crack Initiation*

A considerable amount of work has been conducted in the field of fatigue deformation and crack initiation. Intense slip bands (persistent slip bands) and plastic strain localization occur more readily as a result of cyclic deformation than during monotonic deformation. Fatigue deformation and crack initiation are strongly dependent on microstructure and cyclic slip behavior.[40] Reduction in grain size[5,6,17-19] and introduction of small incoherent particles[25,26] can improve the resistance to FCI, due to slip homogenization and/or slip length shortening.[40] Fatigue cracks nucleate directly at intense slip bands or indirectly by grain boundary cracking, by particle-matrix interface decohesion, or by particle fracture, as dislocation pile-ups reach a critical value.[42]

In the early stage of the LCF tests, all the materials cyclically hardened due to an increase in the dislocation density. As the dislocation density saturated, discrete slip

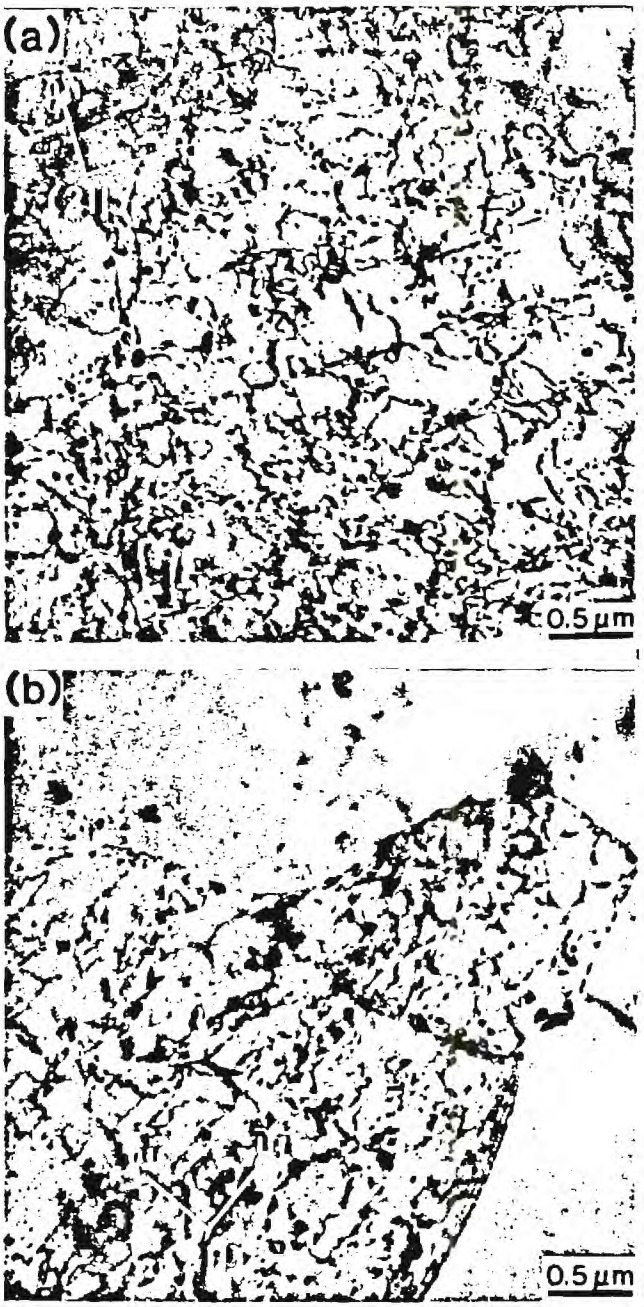

Fig. 6—TEM's showing the planar slip characteristics in the (*a*) IMIP: 2 pct of plastic tensile deformation, (*b*) PMCP: 1.5 pct of plastic tensile deformation, and also showing the dislocation slip extending across the slightly misoriented grain boundaries in (b). (−1° : 1 deg of grain boundary misorientation.)

Table V. Mechanical Properties of the X7091-T651 Materials

	E (GPa)	YS (MPa)	Elong (Pct)	$\ln \frac{A_0}{A}$ (Pct)	n	ε_f'(Pct)	c	n'
IMCP	71*	549	15.9	40	0.053	92	−0.89	0.071
IMIP		543	15.2	37	0.063	16	−0.62	0.075
PMCP		558	14.8	27	0.055	25	−0.74	0.090
PMIP		497	17.7	40	0.065	122	−0.84	0.106

E = Elastic modulus
YS = Proof stress, $\sigma_{0.2}$
$\ln \frac{A_0}{A}$ = Ductility from reduction in area
n = Strain hardening exponent
ε_f' = Fatigue ductility coefficient
c = Fatigue ductility exponent
n' = Fatigue strain hardening exponent
* = Reference 21

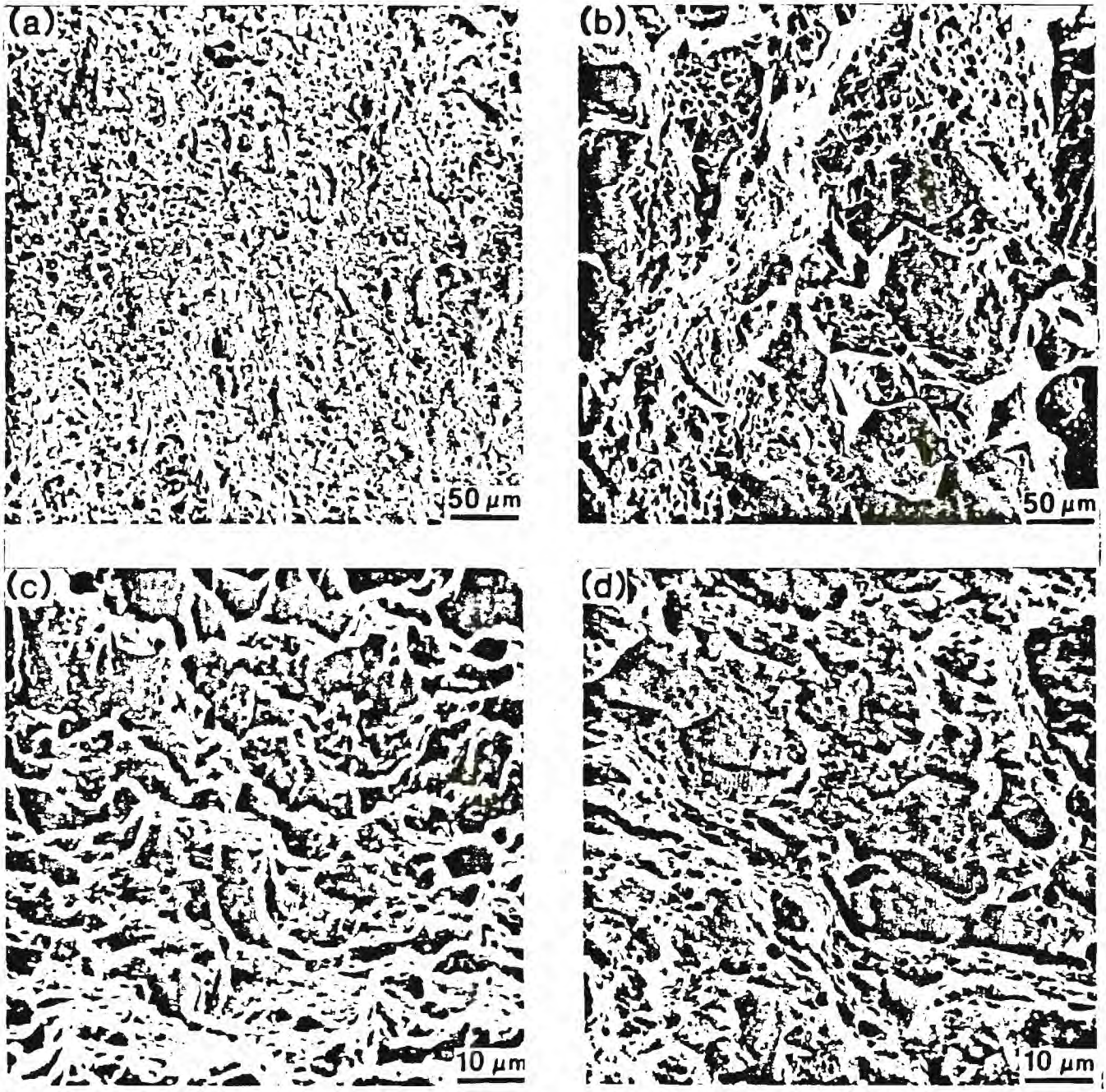

Fig. 7—SEM's of the tensile fractographs showing the fracture features of: (*a*) IMCP, (*b*) IMIP, (*c*) PMCP, and (*d*) PMIP.

bands formed and localized the cyclic strain in the IMIP (Figure 8(b)). Less discrete bands formed in the IMCP material (Figure 8(a)). The homogeneous fine slip observed in the P/M materials was in marked contrast to the coarse bands of the I/M alloys (Figures 8(c) and 8(d)). However, the PMIP alloy showed a tendency toward slip band formation (Figure 8(d)). The degree of strain localization decreased with decreasing grain and particle size and the FCI resistance, defined as the number of reversals to macroscopic crack growth, increased (except for PMCP), in agreement with studies (Figure 9). The PMCP showed the poorest LCF life, even though it had a microstructure conducive for homogeneous deformation. The modified P/M microstructure obtained by ITMT had an FCI resistance either comparable or superior to those of other 7XXX I/M alloys[5,6] and the best of the materials investigated in this study.

Figures 8(a) and 8(c) show that slip bands extend across the slightly misoriented grain boundaries for materials having a sharp texture. Similar extended slip bands were previously observed on fatigue specimen surfaces of sharply textured 7050-T6.[6] Elimination of grain boundaries as effective barriers to slip and a possible increase in slip length may have occurred during fatigue as well as during monotonic deformation. Consequently, the slip in the IMCP was mainly

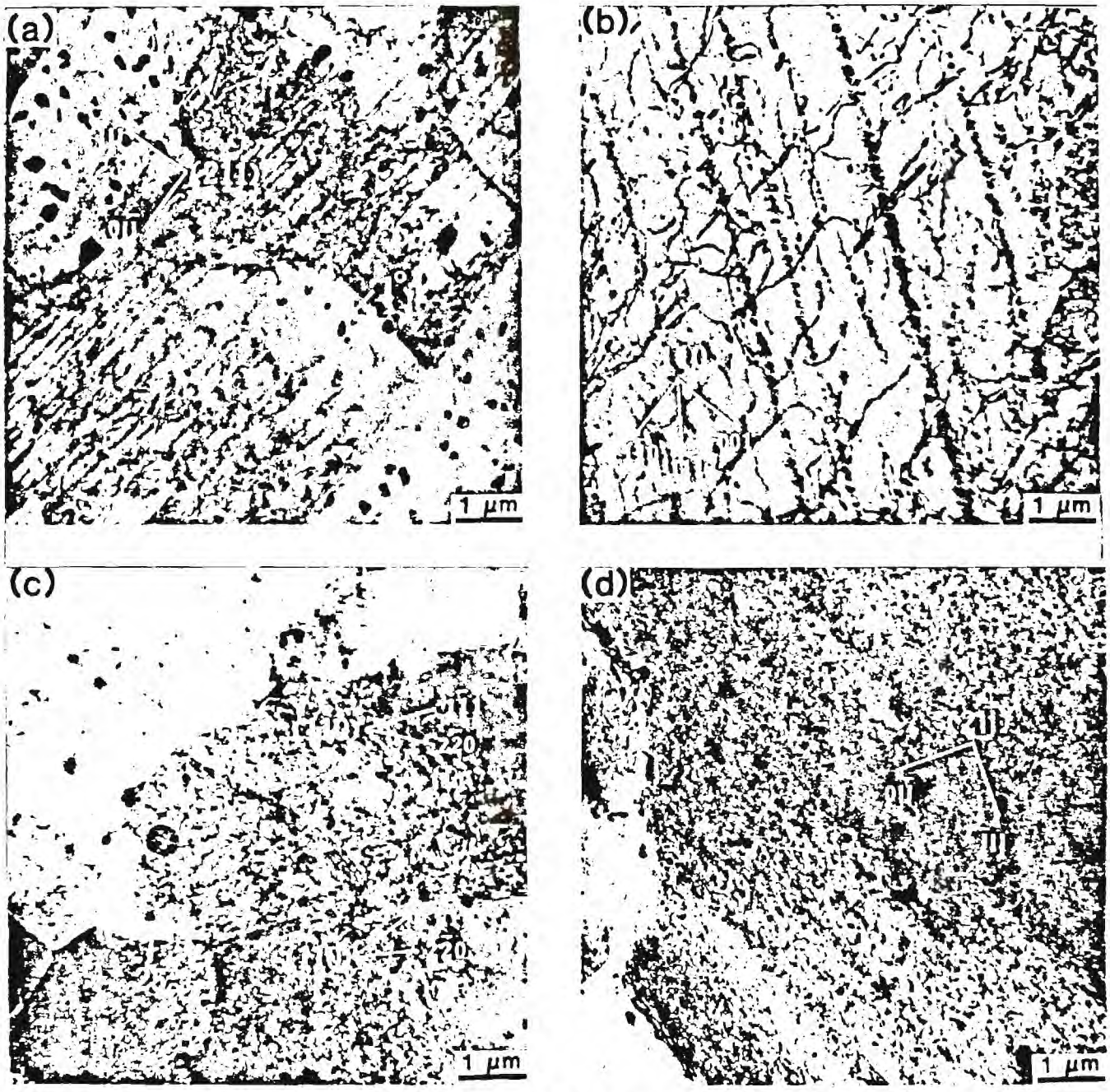

Fig. 8—TEM's showing the fatigue deformation and strain localization in LCF specimens at $\Delta\varepsilon_T/2$ = 1.3 pct: (*a*) IMCP, N_f = 250 cycles; (*b*) IMIP, N_f = 180 cycles; (*c*) PMCP, N_f = 150 cycles; and (*d*) PMIP, N_f = 290 cycles. (−1° : 1 deg of grain boundary misorientation.)

retarded by coarse particle stringers, and fatigue cracks were initiated at slip band/particle intersections or at particles lying along slip bands (Figure 10(a)). Since P/M refined the particle structure, FCI of the PMCP was associated with other detrimental features such as the oxide clusters along particulate interfaces (Figure 10(c)). The sharp texture increased the slip length and raised the stress concentration level at the brittle oxide boundaries. An early crack initiation and poor FCI resistance resulted despite the fine grain and particle structures of the material. Voss[8] also observed a shorter fatigue life for P/M 7075-T6 than for I/M 7075-T6 extrusions in the LCF region.

Fatigue cracks nucleated at slip bands and grain boundaries in the IMIP (Figure 10(b)), most likely due to the material's long slip distance and slip incompatibility across grain boundaries. However, the ITMT dissociated grain boundaries from oxides and produced a weak texture, and fatigue cracks were nucleated at the slip bands on free surfaces of the PMIP (Figure 10(d)).

The FCI resistance was a result of the combined effects of deformation behavior and crack initiation mechanism. Small grain sizes and fine particle distributions acted to homogenize deformation and enhanced the FCI resistance. However, an increase in slip length due to the presence of

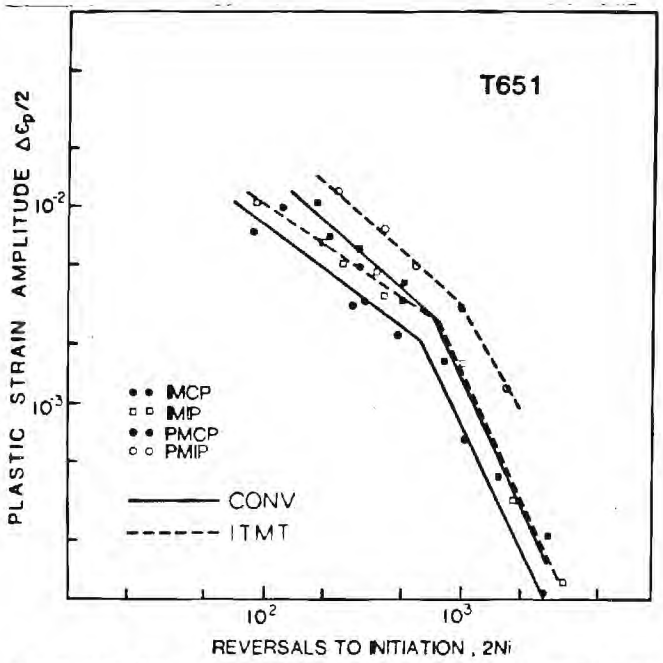

Fig. 9—LCF Coffin-Manson plots for crack initiation in dry air, showing variations in FCI resistance.

a sharp texture raised the stress level at the coarse particles of the IMCP or at weak oxide boundaries of the PMCP, and decreased the FCI resistance below that expected when considering grain size alone. The small recrystallized grain structure, fine particle distribution, weak texture, and the absence of oxides at grain boundaries resulted in the PMIP having the best FCI resistance among all materials. Hirose and Fine[43] reported a similar result for ITMT X7091-type alloy having 0.8 pct Co.

D. *Fatigue Crack Propagation*

The FCGR's of these experimental materials are shown in Figure 11, by plots of da/dN *vs* ΔK. A plateau connects the threshold and Paris regions on the FCGR curve from 10^{-9} to 10^{-8}m per cycle. A study[44] on γ-Fe-Ni-Al alloys indicated that grain boundaries act as effective barriers to slip, and the plateau begins when the static plastic zone size is approximately the same as the grain size and ends when the reverse plastic zone size is as large as the grain size. This argument is not applicable to the FCGR plateaus of these materials, since there is no good correlation between the plastic zone sizes and grain sizes. Similar plateaus have been reported for Al-Zn-Mg-Cu alloys, and their positions vary with environment and deformation behavior.[15] The diffusion rate of the damaging environment, *e.g.*, hydrogen, may determine the FCGR in the plateau region until the accumulation rate of fatigue damage reaches a critical value. The environment has less effect beyond this point, which in our case corresponds to a growth rate of $\sim 10^{-8}$m per cycle.

The FCP resistance was found to be best for the I/M's (ΔK_{th}'s ~ 3.0 MPa $m^{1/2}$), intermediate for the PMIP alloy (ΔK_{th} ~ 2.5 MPa $m^{1/2}$), and worst for the PMCP alloy (ΔK_{th} ~ 2.3 MPa $m^{1/2}$). Hirose and Fine[43] reported that the ΔK_{th} of extruded X7091 P/M alloy with 0.8 pct Co content was 0.9 MPa $m^{1/2}$ in air, while the value of the same alloy with thermomechanical treatment was 1.6 MPa $m^{1/2}$. Our results show a similar trend. The differences in our ΔK_{th}'s and theirs may be due to different testing environments. Several studies[5,6,20,21,42] have suggested that the FCGR's of aluminum alloys decrease with an increase in grain size. This is attributed to the dislocation slip being more reversible,[20] or to less plastic strain being accumulated,[45] or to a greater degree of fatigue crack closure.[46] In the threshold and Paris regions, a grain size dependence was found between the FCGR's of the I/M materials and the PMIP and PMCP materials, but the curves of IMCP and IMIP overlapped. The particle distributions did not produce an obvious effect on either the FCGR's or the fracture surfaces. Previous studies[27,28] have also shown that particles have only a slight effect at low FCGR's ($<10^{-8}$m per cycle).

The fractographic features may be described as follows: Facets with a brittle appearance were observed from the threshold level up to the midpoint of the Paris region. No obvious change in the average size of the facets occurred throughout the facet region, although their appearance varied from material to material (Figure 12). Crystallographic crack propagation, at low growth rates, usually occurs along the [100] directions on (001) planes.[47] Crack propagation progressed in a zigzag fashion in the ITMT materials (Figures 12(b) and 12(d)), possibly due to randomly oriented (001) planes in the materials. The less angular features apparent in the CP materials (Figures 12(a) and 12(c)) were due to approximately parallel orientations of (001) planes. The FCP crack morphology strongly depended on the textures of these materials. Lin and Starke[15] have shown that zigzag FCP has lower FCGR's than a straight FCP path, due to the longer actual path length of the zigzag crack. Beevers,[46] and Minakawa and McEvily[48] have also indicated that the promotion of crack surface roughness increases the degree of crack closure in the low ΔK region, and results in a higher threshold value. Consequently, in addition to the grain size effect, the zigzag crack path may have also affected the FCGR of PMIP. However, these effects do not explain the similar FCGR's of the I/M materials.

Figures 12(b) and 12(d) show that the facets were approximately equivalent to the grain sizes for IMIP and PMIP. In contrast to these weakly textured materials, the facets of IMCP and PMCP were several times larger than their grain dimensions (Figures 12(a) and 12(c)). This suggests that an increase in slip length has probably occurred during FCP of the sharply textured materials. The similar FCGR's of the I/M materials may be accounted for by their similar slip lengths (as discussed in the previous section). The FCP path may still have a secondary effect on the FCGR's of these two alloys. Increase in slip length did not have a pronounced effect on the FCGR of the other sharply textured alloy, PMCP, because this positive effect could not overcompensate for the detrimental effects of brittle oxides at boundaries and homogeneous slip.

A relationship which examines the grain size dependence of FCGR can be applied to the alloys in this study, but the grain size parameters should be modified to consider the actual slip length for materials with a sharp texture. The crack path varied with the texture of the alloy, and contributed a secondary effect on the FCGR. Therefore, the

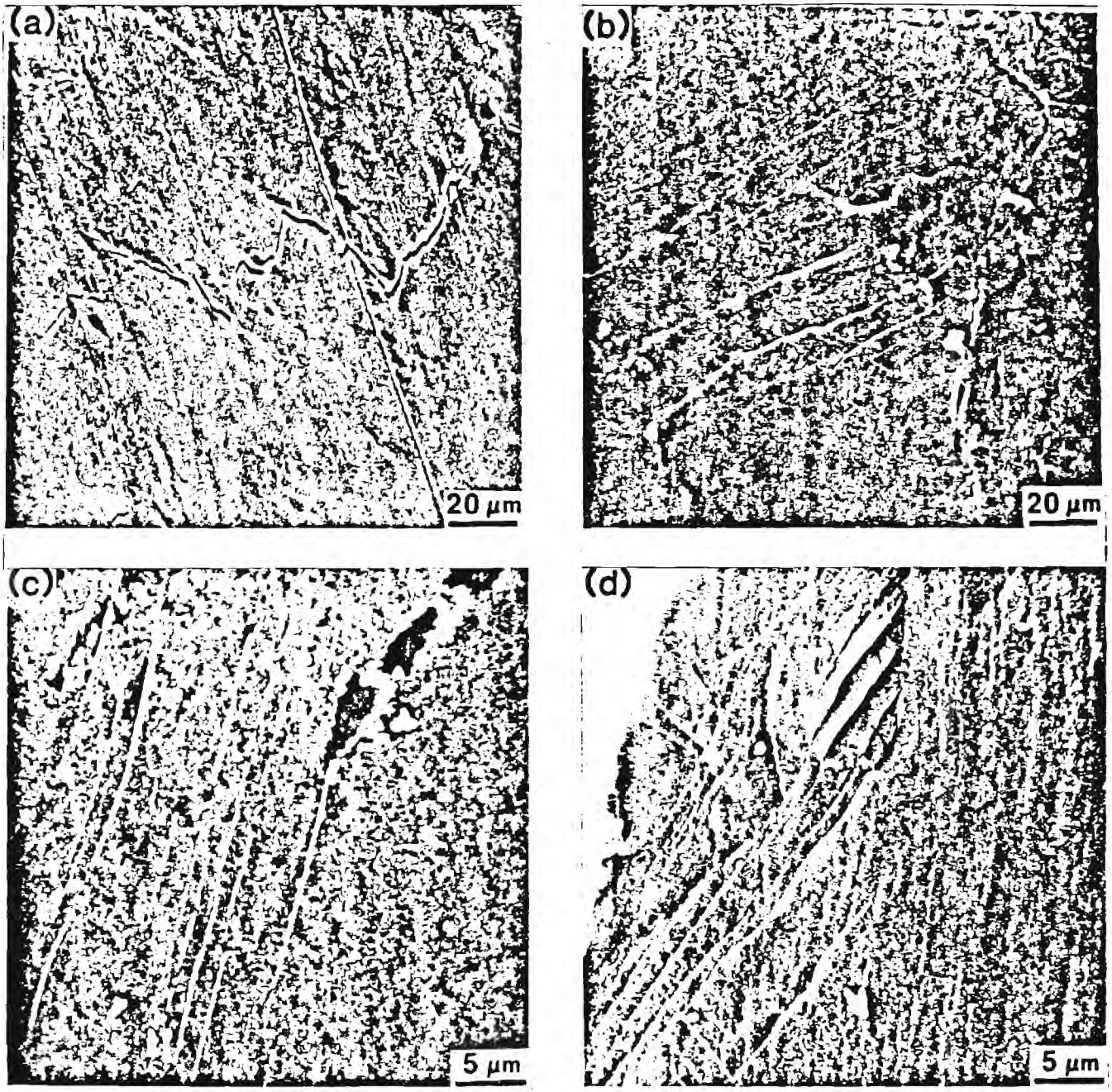

Fig. 10—SEM's showing the surface markings and FCI sites of the LCF specimens, $\Delta\varepsilon_T/2$ = 1.3 pct: (IMCP, N_i = 250 cycles; (*b*) IMIP, N_i = 180 cycles; (*c*) PMCP, N_i = 150 cycles; and (*d*) PMIP, N_i = 290 cycles.

intermediate grain size and the texture-induced zigzag FCP path led to a moderate FCGR for PMIP.

IV. CONCLUSIONS

1. The rapidly solidified powder metallurgy products had finer grain structures and particle distributions than the ingot metallurgy products. Due to the effects of incoherent particles on dislocation generation and on the nucleation of recrystallization, ITMT processing produced a coarser, recrystallized grain structure with a weak texture. This was in contrast to the unrecrystallized grain structure and sharp texture of the conventionally processed materials.
2. Texture had a pronounced effect on the deformation behavior, particularly that of the PMCP material. Slip may extend beyond the slightly misoriented grain boundaries reducing their effectiveness as barriers to slip.
3. The degree of strain localization during fatigue decreased with grain size and particle size and distribution. The FCI resistance increased with a decrease in the degree of strain localization, with the exception of PMCP. The FCI

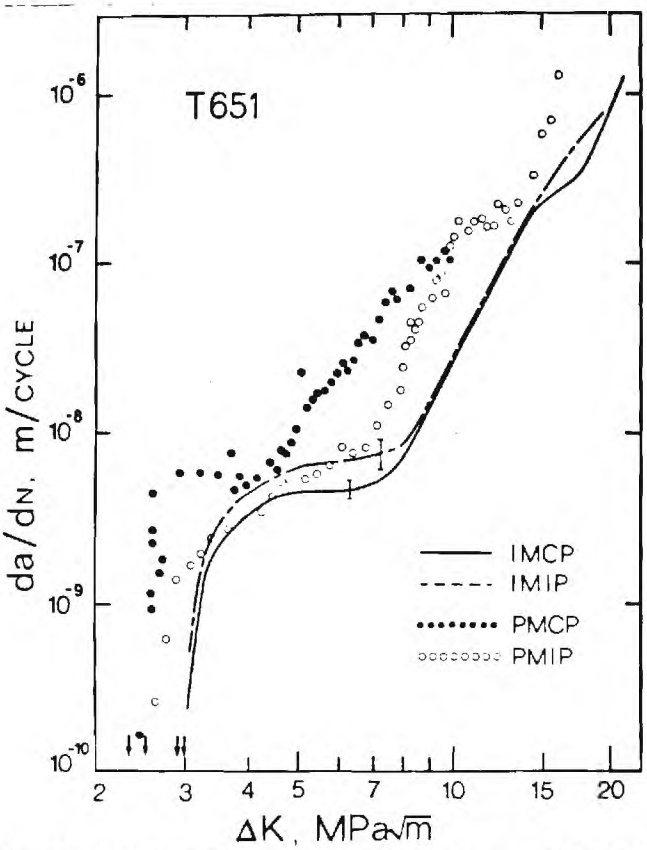

Fig. 11—FCGR's of the experimental alloys in dry air, with $R = 0.1$, 10 Hz.

sites were located at the most detrimental features in each alloy, such as: at slip bands on free surfaces for PMIP, at particle stringers for IMCP, and at highly misoriented grain boundaries and long slip bands for IMIP. The oxide-induced intergranular FCI, enhanced by the effect of a sharp texture, contributed to the poor FCI resistance of the PMCP alloy.

4. The FCGR's demonstrated a dependence of grain size (or slip length). It is believed that a large grain size allows a greater amount of reversible slip and thus reduces the amount of accumulated plastic strain within the reverse plastic zone. The texture dependence of the FCP path had a secondary effect on the FCGR's of these alloys, with a "zigzag" crack path decreasing the FCGR's of the materials having a weak texture. The fatigue crack closure effect may also be involved in both cases.
5. ITMT of the X7091 powder alloy produced an optimum microstructure for the best overall mechanical properties. The homogeneous deformation in this alloy, associated with the small grain size, fine particle distribution, and weak texture, resulted in monotonic properties which were comparable to those of the other alloys and a superior FCI resistance. The moderate slip length and the texture-induced FCP path showed an intermediate FCGR.

ACKNOWLEDGMENTS

This work was sponsored by the Army Research Office under Contract No. DAAG29-80-C-100. The support of George Mayer, Program Manager, is deeply appreciated.

REFERENCES

1. E. DiRusso, M. Conserva, M. Buratti, and F. Gatto: *Mater. Sci. & Eng.*, 1974, vol. 14, p. 23.
2. J. Waldman, H. Sulinski, and H. Markus: *Metall. Trans.*, 1974, vol. 5, p. 573.
3. B. K. Park and J. E. Vruggink: *Thermomechanical Processing of Aluminum Alloys*, J. G. Morris, ed., TMS-AIME, Warrendale, PA, 1978, p. 25.
4. E. A. Starke, Jr.: *Mater. Sci. & Eng.*, 1977, vol. 29, p. 99.
5. R. E. Sanders, Jr. and E. A. Starke, Jr.: *Thermomechanical Processing of Aluminum Alloys*, J. G. Morris, ed., TMS-AIME, Warrendale, PA, 1978, p. 50.
6. R. E. Sanders, Jr. and E. A. Starke, Jr.: *Metall. Trans. A*, 1978, vol. 9A, p. 1087.
7. F. F. Gurney, D. J. Abson, and V. DePierre: *Powder Metallurgy*, 1974, vol. 17, no. 33, p. 46.
8. D. P. Voss: Final Report, AFOSR 77-3440, EOARD-TR-79-1, October 1979.
9. J. P. Lyle, Jr. and W. S. Cebulak: *Met. Eng. Quart.*, 1974, vol. 14, no. 1, p. 52.
10. J. P. Lyle, Jr. and W. S. Cebulak: *Metall. Trans. A*, 1975, vol. 6A, p. 685.
11. W. S. Cebulak, E. W. Johnson, and H. Markus: *Met. Eng. Quart.*, 1976, vol. 16, no. 4, p. 37.
12. G. Lütjering and S. Weissman: *Acta Metal.*, 1970, vol. 18, p. 785.
13. K. M. Carlsen and R. W. K. Honeycombe: *J. Inst. of Metals*, 1954-55, vol. 83, p. 449.
14. F. S. Lin and E. A. Starke, Jr.: *Mater. Sci. & Eng.*, 1979, vol. 39, p. 27.
15. F. S. Lin and E. A. Starke, Jr.: *Mater. Sci. & Eng.*, 1980, vol. 45, p. 153.
16. M. Peter and G. Lütjering: Z. *Metallkd.*, 1976, vol. 67, p. 811.
17. R. E. Sanders, Jr. and E. A. Starke, Jr.: *Mater. Sci. & Eng.*, 1977, vol. 28, p. 53.
18. G. Lütjering, T. Hamajima, and A. Gysler: *Proc. of 4th International Conf. on Fracture*, Waterloo, Canada, D. M. R. Taplin, ed., Pergamon Press, NY, 1977, vol. 2, p. 7.
19. G. Terlinde and G. Lütjering: *Metall. Trans. A*, 1982, vol. 13A, p. 1283.
20. J. Lindigkeit, G. Terlinde, A. Gysler, and G. Lütjering: *Acta Metal.*, 1979, vol. 27, p. 1717.
21. R. E. Sanders, Jr., W. L. Otto, Jr., and R. J. Bucci: AFML-TR-79-4131, September 1979.
22. M. F. Ashby: *Strengthening Methods in Crystal*, A. Kelly and R. B. Nicholson, eds., Applied Science Publishers, London, 1971, p. 122.
23. R. H. Van Stone, R. H. Merchant, and J. R. Low, Jr.: *Fatigue and Fracture Toughness–Cryogenic Behavior*, TMS-AIME, Warrendale, PA, 1974, p. 93.
24. J. T. Staley: *Properties Related to Fracture Toughness*, ASTM STP 605, W. R. Warke, V. Weiss, G. Hahn, eds., ASTM, Philadelphia, PA, 1976, p. 71.
25. E. E. Hornbogen and G. Lütjering: *Proc. of 6th International Conf. on Light Metals*, Aluminium Verlag, Germany, 1975, p. 40.
26. G. Lütjering, H. Doker, and D. Munz: *Proc. of 3rd International Conf. on Strength of Metals and Alloys*, Iron and Steel Institute, London, 1973, p. 427.
27. D. Broek: *Proc. of 2nd International Conf. on Fracture*, P. L. Pratt, ed., Chapman and Hall, London, 1969, p. 754.
28. S. M. El-Soudani and R. M. Pelloux: *Metall. Trans.*, 1973, vol. 4, p. 519.
29. G. E. Dieter: *Mechanical Metallurgy*, 2nd ed., McGraw-Hill, Inc., New York, NY, 1976, p. 193.
30. I. G. Palmer, R. E. Lewis, and D. D. Crooks: *Aluminum-Lithium Alloys*, T. H. Sanders, Jr. and E. A. Starke, Jr., eds., TMS-AIME, Warrendale, PA, 1981, p. 241.
31. T. H. Sanders, Jr.: Naval Air System Command Contract No. N00019-77-0499, Final Report, June 1980.
32. J. A. Wert, N. E. Paton, C. H. Hamilton, and M. W. Mahoney: *Metall. Trans. A*, 1981, vol. 12A, p. 1267.
33. E. E. Underwood and E. A. Starke, Jr.: *Fatigue Mechanics*, ASTM STP 675, J. T. Fong, ed., ASTM, Philadelphia, PA, 1979, p. 633.
34. E. Nes: *Acta Metal.*, 1976, vol. 26, p. 391.
35. J. A. Walker and E. A. Starke, Jr.: unpublished research, 1982.
36. H. Hu, R. S. Cline, and S. R. Goodman: *Recrystallization, Grain Growth and Textures*, ASM, Metals Park, OH, 1966, p. 295.

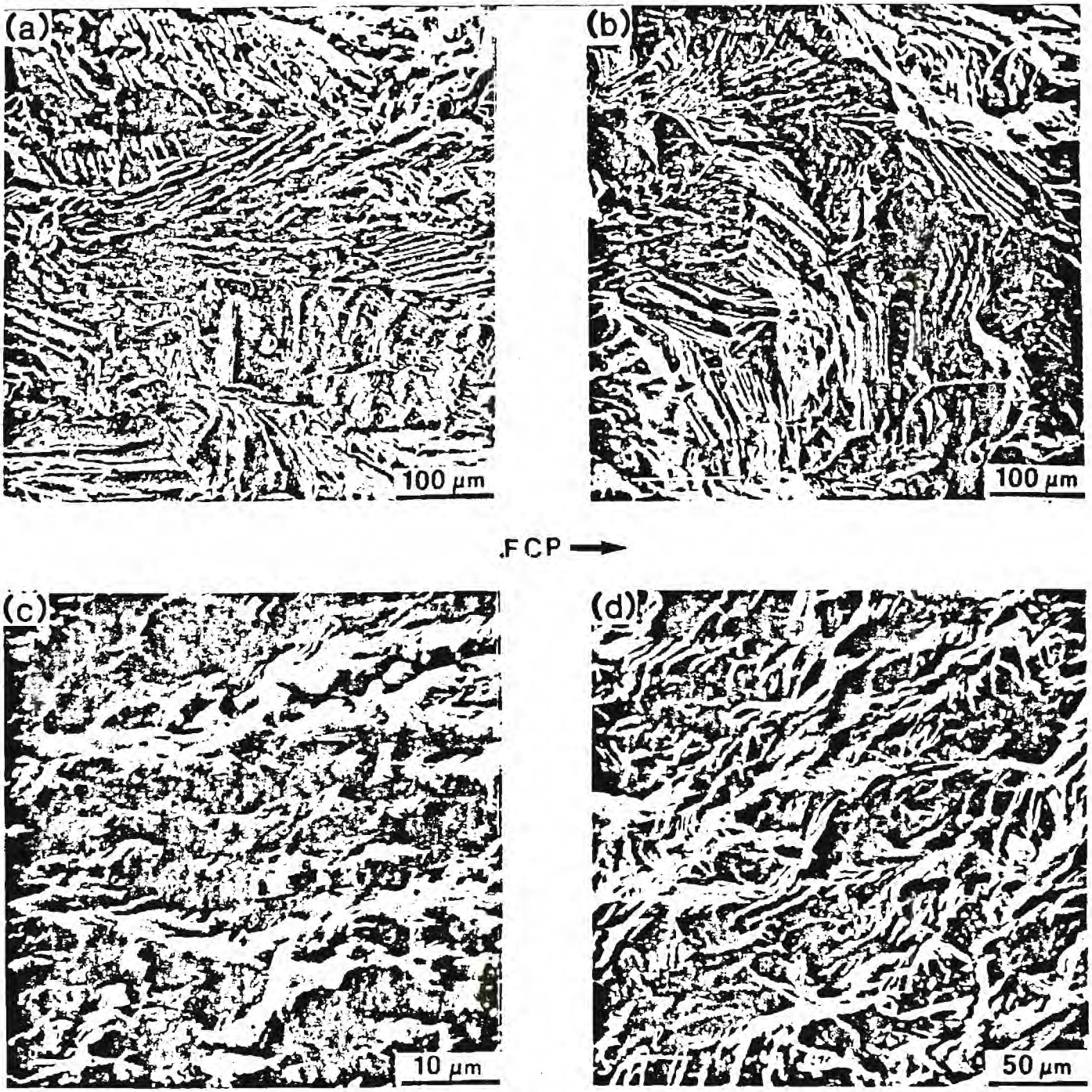

Fig. 12—SEM's of the FCP fracture features at $da/dN = 10^{-8}$ m per cycle: (*a*) IMCP, (*b*) IMIP, (*c*) PMCP, and (*d*) PMIP; *l* is the grain dimension along the FCP direction.

37. K. Brown: *Metall. Trans.*, 1971, vol. 2, p. 2983.
38. R. W. Chan: *Proc. Phys. Soc.*, 1950, vol. 63A, pt. 1, p. 323.
39. E. A. Calnan and C. J. B. Clews: *Phil. Mag.*, 1951, vol. 42, p. 616.
40. E. A. Starke, Jr. and G. Lütjering: *Fatigue and Microstructure*, ASM, Metals Park, OH, 1978, p. 205.
41. A. W. Thompson: *Work Hardening in Tension and Fatigue*, A. W. Thompson, ed., TMS-AIME, Warrendale, PA, 1977, p. 89.
42. M. E. Fine: *Metall. Trans. A*, 1980, vol. 11A, p. 365.
43. S. Hirose and M. E. Fine: Fatigue Crack Initiation and Propagation in High Strength P/M Alloys, *Metall. Trans. A*, in press.
44. E. Hornbogen and K. H. Zum Gahr: *Acta Metal.*, 1976, vol. 24, p. 581.
45. S. B. Chakrabortty: *Fatigue of Eng. Mater. and Structures*, 1979, vol. 2, p. 331.
46. C. J. Beevers: *Preliminary Proc. from International Symp. on Fatigue Thresholds*, arranged by the Aeronautical Res. Inst. of Sweden and the Swedish Plastics and Rubber Inst., Stockholm, Sweden, 1981, vol. 1, no. 17.
47. C. Q. Bowles and D. Broek: *Int. J. Fracture Mechanics*, 1972, vol. 8, p. 75.
48. K. Minakawa and A. J. McEvily: *Preliminary Proc. from International Symp. on Fatigue Thresholds*, arranged by the Aeronautical Res. Inst. of Sweden and the Swedish Plastics and Rubber Inst., Stockholm, Sweden, 1981, vol. 2, no. 36.

Final Report

LOW DENSITY ALUMINUM ALLOY DEVELOPMENT PROGRAM

Air Force Contract No. F33615-81-C-5053

To

Boeing Commercial Airplane Company
P.O. Box 3707
Seattle, Washington 98124

From

K. M. Bresnahan, R. T. Chen and E. A. Starke, Jr.
Fracture and Fatigue Research Laboratory
Georgia Institute of Technology
Atlanta, Georgia 30332

January 17, 1983

Georgia Tech E-19-668

ABSTRACT

Study of the RS alloys comprised of inert gas atomized powder from Pratt & Whitney Aircraft has been centered on Alloys No. 1 and 2. Samples of extruded bars were examined in the as-received and SHT conditions. Microstructural features were revealed by electropolish and bromine etching techniques. A relatively large volume fraction of precipitate phase intermetallic particles was evident in the as-received condition. Solution heat treatment at 811K for 0.5 hr. provided the best results; however, a significant amount of precipitate phase particles remained in the microstructures. Based on morphology and x-ray diffraction data, the precipitate phase particle distribution is at least trimodal.

Tensile tests performed on all seven RS alloys in the SHT condition demonstrated relatively low ductility. Examination of tensile fracture surfaces revealed a large number of precipitate phase particles on the surfaces, apparently intact. The precipitate phase-aluminum matrix interface seems to be involved in the crack initiation and propagation processes.

Microstructural features and x-ray data indicate that the precipitate phases are present in the RS powder prior to extrusion. A fine dendritic microstructure exists in the unprocessed RS powder, with no precipitate phase particles apparent at magnifications up to 6000 diameters after a sodium hydroxide etch. Diffraction lines resulting from precipitate phases do appear in DeBye-Scherrer measurements on the unconsolidated RS powder. Heat treatment of unconsolidated powder results in a breakdown of the fine dendritic structures and apparent coarsening of precipitate phase particles. In the extruded material, fragmented precipitate phase particles are evident indicating

their formation prior to extrusion. Based on the information developed at this time, the formation of precipitate phase particles as they appear in the extruded samples is occurring during the extrusion preheat treatment. Optimization of this preheat treatment may significantly improve the mechanical properties of these alloys by changing the precipitate phase particle type, size and distribution.

The alloy with nominal composition Al-2.5Li-1.5Cu-1.0Mg, produced by INCO's mechanical alloying process, has been studied. A fine grained microstructure with finely distributed, equiaxed particles is apparent in this alloy. The monotonic and cyclic mechanical properties were investigated in an appropriate SHT and aged condition. This treatment involved SHT at 811K for 0.5 hr, stretching to 2% total strain, followed by natural aging for 48 hrs and artificial aging at 463K. High strength and low ductility are demonstrated by this alloy. The high strength and low ductility is associated with a high volume fraction of particles and dense substructure. Low cycle fatigue properties of this alloy in the naturally aged condition show initial softening at the first cycle, followed by cyclic hardening. The initial softening is due to residual stress relief. Cyclic hardening is associated with dislocation-particle interaction.

LOW DENSITY ALUMINUM ALLOY DEVELOPMENT PROGRAM

Annual Report
January 1 - December 31, 1982

PHASE II, Task I - Quantitative Microstructural Analysis and Mechanical Property Correlations

INTRODUCTION

The primary objective of this research program is to develop new aluminum-lithium (Al-Li) alloys with significantly lower density and greater specific modulus and strength relative to existing alloys. This effort is being performed in accordance with United States Air Force Contract F33615-81-12-5053 presented in Technical Proposals D6-49955-1 and D6-49955-2 by the Boeing Military Airplane Company. Literature reviews and the preparation of a formal research proposal were completed prior to receiving the first alloy samples in August. The work has been centered on alloys produced by powder metallurgy (P/M) techniques, involving mechanical alloying (MA) and inert gas atomization (rapid solidification, RS) processes. The ultimate goal of this program is to develop high performance aluminum alloys with optimized density, strength, and stiffness for application as airframe components.

The extremely high cooling rates (10^4 to 10^6 K/sec) achieved during RS processing generally result in a refinement of microstructural features, which can lead to improved mechanical properties when compared to ingot cast alloys. In the Al-Li system, the benefits of lower density and higher elastic modulus have been offset by reduced ductility, fracture toughness and stress corrosion cracking resistance. Improvement of these properties has been hindered by basic physical and mechanical metallurgical constraints. Segregation of lithium in slowly solidified cast ingots ultimately contributes to

low fracture toughness, and one of the most significant effects of rapid solidification processing is a reduction or elimination of segregation effects during solidification.

In a typical mechanical alloying process, constituent powder particles are repeatedly fractured and cold welded by the continuous impacting action of a milling medium. Composite powder particles are formed, with a composition corresponding to the percentages of the elements in the initial charge. The composite powders produced in this manner are characteristically dense, cohesive and homogeneous. Increased strength in MA alloys is attributed to the uniform distribution of fine dispersoids such as oxides and carbides achieved in the consolidated condition.

The graduate student selected to participate in this research project is Keith M. Bresnahan. A literature review has been conducted, and the results presented in a M.S. thesis reserach proposal. The scope of this proposal included the characterization of microstructures, deformation and fracture modes of new Al-Li alloys.

Alloy samples of three different nominal compositions produced by INCO's proprietary mechanical alloying process were received August 23, 1982, and seven powder metallurgy alloys comprised of inert gas atomized powder from Pratt & Whitney Aircraft arrived September 14. The compositions of these alloys are given in Table 1. Two of the rapidly solidified powder metallurgy alloys and one of the MA alloys have been selected and approved as the subject of the initial investigation in this research project. The rapidly solidified alloy samples are rectangular extrusions, measuring approximately 18 mm x 65 mm x 610 mm including a 1-3 mm thick periphery of canning aluminum

(6061). The MA Alloy samples are rectangular extrusions, measuring 13 mm x 51 mm x 305 mm (including the can). In the as-received condition, these samples were not solution heat treated or stretched. Samples of unconsolidated RS powder were received for alloys No. 1 and 2 in December.

EXPERIMENTAL PROCEDURES

Rapidly Solidified Alloys

Identification of the phases present in the alloys under study is being established mainly through the use of transmission electron microscopy (TEM) and x-ray diffraction techniques. TEM is essential in the examination of the fine microstructural constituents. Bright-field and dark-field imaging is employed to observe shape, size and distributional characteristics of the precipitate particles. Selected area diffraction can be used to develop a correlation between the features observed through imaging techniques and the crystallography of the specimen. X-ray diffraction patterns from powder samples are being recorded in a DeBye Scherrer camera, and diffractometer scans were recorded on the extruded material in the as-received and SHT conditions. Subsequent measurement of diffraction angles related to the diffraction lines on the film or scan chart, and calculation of the planar spacing (d) generating the diffraction results in data which can be compared with d values from patterns of known materials. Internal standards are used to establish the camera constant for each exposure. The diffractometer was a Norelco unit equipped with a Phillips copper K_α x-ray source.

Optical microscopy is useful in determining the precipitate particle shape, size, and distribution, and other microstructural features of sufficient

size (i.e., large inclusions, porosity, etc.) Bromine etching and electropolishing techniques have been used to reveal microstructural features in two alloys presently under study (Numbers 1 and 2). The bromine etching procedure involved submersing samples in a boiling solution of 10% bromine in methanol for 60 seconds. This solution selectively attacks the aluminum matrix exposing intermetallic particles in relief, while grain and subgrain boundaries are also revealed due to extreme susceptibility to the etchant. The bromine-etched surfaces were examined in a Cambridge scanning electron microscopy (SEM). Electropolishing was performed in a 1:2 solution of nitric acid in methanol at 253K (-20^{o}C). An electric potential of 12 volts was applied for 15 to 30 seconds, during the polishing procedure.

A small amount of unconsolidated RS powder was cast in epoxy, ground and polished, and examined optically. The metallic powder sample was etched in a solution of 10 grams sodium hydroxide in 90 milliliters of water at 343K for 1 minute. The sample was then desmutted in a 50% nitric acid solution in water. A small section of the epoxy mount containing several etched powder particles was removed and fixed to an aluminum pedestal with copper print. The powder sample and pedestal were then covered with a very thin, conductive layer of gold palladium by sputter coating, and the powder particles were examined with a scanning electron microscope.

Cylindrical tensile samples were prepared for alloys No. 3 through 7 in the solution heat treated (SHT) condition at 773K for 30 minutes. Tensile samples were also prepared for alloys No. 1 and 2 in the SHT condition at 811K for 30 minutes. The yield stress, fracture stress and total elongation were determined, and the results are shown in Table 2. The tests were performed on

a hydraulic Material Testing System (MTS) machine at a strain rate of 5×10^{-3} cm/sec .

In order to optimize the size and distribution of the precipitate phase particles, heat treatments at various temperatures for different lengths of time have been applied to loose powder samples. Subsequent microstructural analysis should establish the precipitate phase particle size and distribution. To reduce oxide formation on the powder particle surfaces during heat treatment, the powder was wrapped in tantalum foil and vacuum encapsulated. Some powder samples were heat treated in a tantalum boat in an argon atmosphere.

Mechanically Alloyed Alloy

Solutionizing heat treatment was performed in a salt bath followed by artificial aging in an oil bath. The heat treatment schedule is given in Table 3. Cylindrical tensile samples were prepared and pulled on an MTS machine at a strain rate of 2×10^{-3} cm/sec. Low cycle fatigue specimens with 4 mm diameter and 10 mm gage length were polished to 1 micron finish before fatigue testing. Strain controlled fatigue tests were performed on the MTS machine with a strain rate of 2.5×10^{-3} cm/sec. To characterize the particle and grain sizes thin foils were prepared and examined with a TEM at 100 kv. Fracture surfaces were examined using a SEM.

EXPERIMENTAL RESULTS

Rapidly Solidified Alloys

Alloy No. 1 was examined in the following conditions: as-received, SHT at 763K (490°C) for 30 minutes, SHT at 811K (538°C) for 30 minutes, and SHT at 811K for 240 minutes. In the as-received condition, a high volume fraction

of particles was evident, Figure 1. Based on morphology, the particle distribution was at least trimodal; consisting of roughly spherical, plate, and irregular shapes. The largest particles apparent by this analytical technique were approximately 12 microns in longest dimension, and the smallest was on the order of .2 microns. Some of the larger particles had fractured with the fragments separating in the extrusion direction, Figure 2, indicating that this deformation occurred during the extrusion process and that these particles existed prior to extrusion. Although a significant decrease in apparent particle volume fraction was evident after the 30 minute solution heat treatments, a relatively high volume fraction remained in the microstructure, Figure 3. No significant particle coarsening occurred during these shorter heat treatments. During the 240 minute SHT at 811K, a considerable reduction in particle volume fraction was observed relative to the shorter heat treatments, however, the plate-shaped particles coarsened up to approximately 20 microns in size, Figure 4. Blistering due to incipient melting and out gassing was also evident after this heat treatment.

Alloy No. 2 exhibited particle distributions and SHT responses similar to alloy No. 1. Since the only difference in these alloys is the .18 weight percent chromium added as a dispersoid forming element, these similarities were anticipated. Although both alloys had uniform particle distributions in general, streaked regions oriented parallel to the extrusion direction were evident in the as-received condition where larger particles were found but very few smaller particles existed, Figure 5. Also, many particles were located on grain and subgrain boundaries.

Diffractometer scans were performed on the as-received and the 30-minute SHT conditions of these two alloys, to begin the precipitate phase identifi-

cation process. Most of the diffraction peaks resulting from the precipitate phase particles in the as-received condition were greatly suppressed by the 811K SHT for 30 minutes. The powder diffraction data files were reviewed to determine which intermetallic compounds had d-spacings corresponding to those determined from the diffractometer measurements. The following compounds have d-spacings corresponding to the diffractometer data: AlLi (δ phase), Al_6CuLi_3 (T_2 phase), Al_5CuLi_3 (R phase), and Al_2Cu. Some of the diffraction peaks evident in the diffractometer scans did not correspond to d-spacings in the available powder diffraction data files and other analytical means will be employed to identify the phases causing these diffraction peaks. Iron-rich particles were discovered with a Kevex energy dispersive fluorescence spectrometer which may be Al_7Cu_2Fe. Quantitative analysis of Kevex data developed from extracted precipitate phase particles may be performed to aid in the phase identification. Transmission electron diffraction will also be used to characterize these phases.

DeBye-Scherrer diffraction measurements performed on samples of unconsolidated RS powder in various heat treated conditions revealed the presence of δ, T_2 and R phases. Diffraction lines corresponding to the d-spacings associated with these phases were also generated by as-received RS powder, indicating that these phases are forming during solidification. After heat treatment at 473K for 90 minutes, δ' (Al_3Li) diffraction lines appeared in the film exposures. This phase was not evident after heat treatment at higher temperatures and longer times. The appearances of the microstructure of the unconsolidated powder after heat treatment at 473K for 90 minutes and at 655K for 300 minutes are shown in Figure 6 compared to the as-received condition. The fine dendritic structure coarsens and begins to break down with increasing

The fine dendritic structure coarsens and begins to break down with increasing heat treatment temperature and time, and the interdendritic precipitate phase particles also coarsen.

Mechanically Alloyed Alloy

The MA Alloy studied had the following nominal composition, Al-2.5Li-1.5Cu-1.0Mg. A fine grained microstructure was exhibited with finely distributed equiaxed particles as shown in Figure 7. SHT resulted in a reduction of precipitate phase particle volume fraction. Grain size in this alloy ranged from 0.5 micron to 1.0 micron.

The hardness peaked rapidly during artificial aging, making it difficult to control the structure in an underaged condition. Table 3 lists the tensile properties of samples with different aging schedules. Although the yield strength was improved by artificial aging, the ductility was severely reduced. The extent to which the fracture occurs in an intergranular or transgranular mode remains undetermined at this time. It is likely that the particle interfaces are the crack path of least resistance, and this could be a contributing factor in the low ductility of this MA alloy.

The presence of Al_4C_3 has been confirmed by x-ray diffraction analysis, but Al_2O_3 peaks were not obtained in the x-ray analysis. The Al_2O_3 may be present in an amorphous form. Further particle characterization will require electron diffraction and energy dispersive x-ray analysis (Kevex).

To address the problem of low ductility, naturally aged specimens were selected for low cycle fatigue (LCF) testing. Figure 8 shows the LCF cyclic response. For a total strain amplitude below 1%, softening was observed in the first cycle, and cyclic hardening followed until saturation was reached. The

cyclic and monotonic stress-strain curves are shown in Figure 9. The cyclic hardening exponent, n', can be expressed as:

$$\sigma_a = \sigma_f' (\frac{\Delta \varepsilon_p}{2})^{n'}$$

where σ_a is the stress amplitude and σ_f' is the fatigue strength coefficient. It was found that the cyclic hardening exponent was very close to the monotonic strain hardening exponent for this alloy. Fractographs of the fatigue fractured samples are shown in Figure 10, and the features exhibited here are similar to that of the tensile fracture surfaces.

A Coffin-Manson (C-M) plot of the LCF test is given in Figure 11. The results follow the C-M relationship which can be expressed as:

$$\frac{\Delta \varepsilon_p}{2} = \varepsilon_f' (2N_f)^{-c}$$

where $\Delta \varepsilon_p$ is the plastic strain range, ε_f' is the fatigue ductility coefficient, $2N_f$ is the number of reversals to failure and c is the fatigue ductility exponent. The exponent c can be estimated from the C-M plot, and a value of $c = 0.5$ was obtained. No break point was observed in the C-M plot, and this indicates that the deformation and fracture modes are similar at high and low strain amplitudes.

CONCLUSIONS

Rapidly Solidified Alloys No. 1 and 2

A relatively high volume fraction of precipitate phase intermetallic particles are evident in the as-received extruded material. Although solution heat treatment at 811K for 0.5 hr reduces the amount of precipitate phase particles, a significant amount remains in the microstructure. SHT for periods longer than 0.5 hr results in significant particle coarsening.

Preliminary x-ray diffraction data indicates the presence of several precipitate phases common in Al-Li-Cu-Mg alloys, however, some of the diffraction data does not correspond to any alloy listed in the powder diffraction data files.

Failure in tensile tests most probably results from crack initiation at the interface between the precipitate phase particles and the aluminum matrix. Low ductility in the SHT condition may be the result of strain localization at the precipitate phase particles.

The precipitate phase particles are present in the RS powder, although they are very small and finely dispersed. Development of the large precipitate phase particles evident in the extruded powder is occurring during the extrusion preheat treatment.

Mechanically Alloyed Alloy

High strength and low ductility are demonstrated by this alloy. The high strength and low ductility is associated with a high volume fraction of particles and dense substructure. Low cycle fatigue properties of this alloy in the naturally aged condition show initial softening at the first cycle, followed by cyclic hardening. The initial softening is due to residual stress relief. Cyclic hardening is associated with dislocation-particle interaction.

TABLE 1. Nominal Chemical Composition for First Iteration Alloys

ALLOY TYPE	ALLOY NO.	ALLOYING ELEMENT (WT.%) Al	Li	Cu	Mg	Zn	Zr	Ca	Cr	O	C
CLASS I ALLOYS PRODUCED BY PRATT & WHITNEY FROM INERT GAS ATOMIZED POWDER											
I	1	Bal.	4.0	3.0	1.5	---	0.2	---	---	---	---
	2	Bal.	4.0	3.0	1.5	---	0.2	---	0.18	---	---
II	3	Bal.	3.0	---	5.5	---	0.2	---	---	---	---
	4	Bal.	3.5	---	10.0	---	0.2	---	---	---	---
III	5	Bal.	1.5	2.0	2.0	7.0	0.2	---	---	---	---
	6	Bal.	3.0	2.0	2.0	7.0	0.2	---	---	---	---
IV	7	Bal.	3.0	2.0	1.0	---	0.2	---	---	---	---
CLASS II ALLOYS PRODUCED BY INCO FROM MECHANICALLY ALLOYED POWDER											
	1	Bal.	2.5	---	2.5	---	---	---	---	0.6	1.1
	2	Bal.	1.5	---	4.0	---	---	---	---	0.6	1.1
	3	Bal.	2.5	1.5	1.0	---	---	---	---	0.6	1.1

TABLE 2. Tensile Properties in the SHT Condition

ALLOY NO.	YIELD STRESS MPa	FRACTURE STRESS MPa	ELONGATION %
1	195	350	7.5
2	222	333	5.3
3	351	462	7.5
4	328	372	2.6
5	290	468	10.0
6	222	300	3.8
7	156	309	5.9

TABLE 3. Heat Treatments and Tensile Properties

SOLUTIONIZING SCHEDULE	AGING SCHEDULE	YIELD STRENGTH	ELONGATION
811K/0.5 hr	RT aging/48 hrs	460 MPa	4.4%
811K/0.5 hr	2% stretch + RT aging/48 hrs + 463K aging/0.5 hr	636 MPa	1 %
811K/0.5 hr	2% stretch + RT aging/48 hrs + 463K aging/4 hrs	535 MPa	1.8%

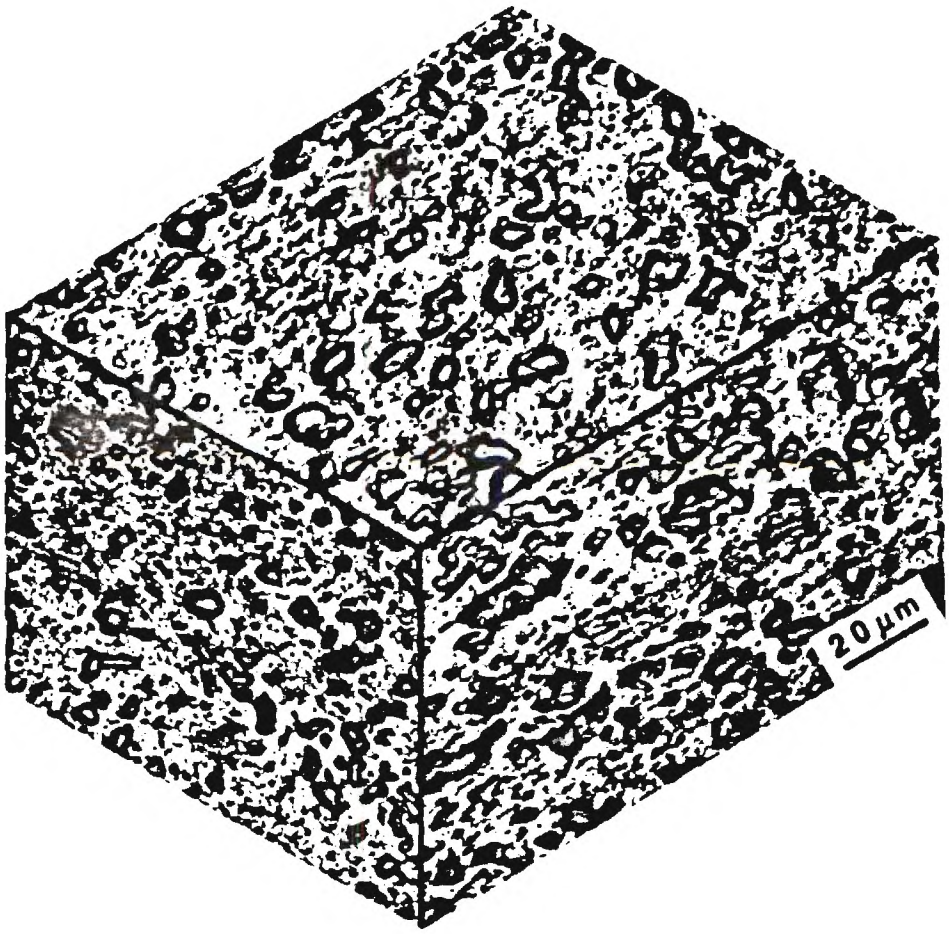

FIGURE 1. Optical micrographs of electropolished extruded alloy no. 1 in the as-received condition.

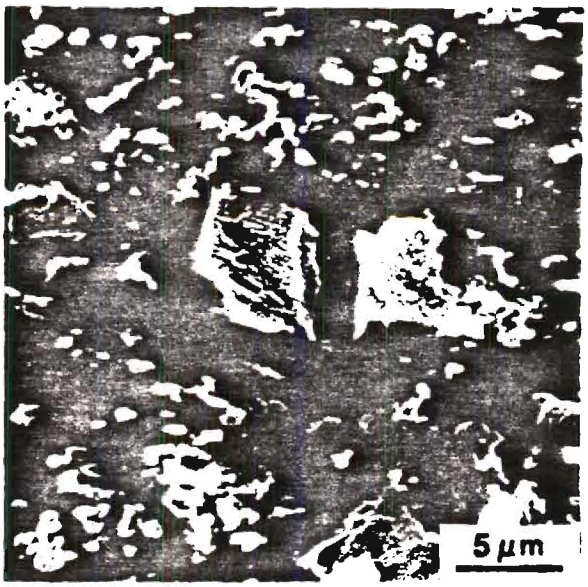

FIGURE 2. Scanning electron micrograph of bromine etched extruded alloy no. 2.

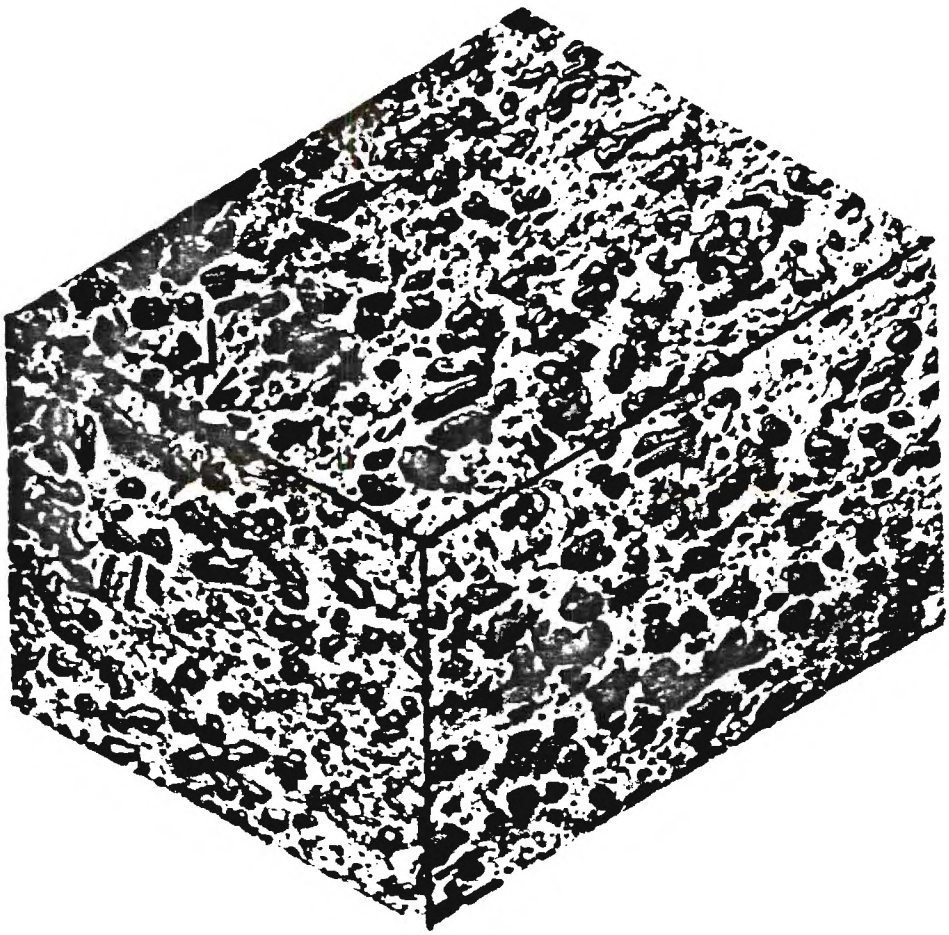

FIGURE 3. Optical micrographs of electropolished extruded alloy no. 1 SHT at 763K for 0.5 hr.

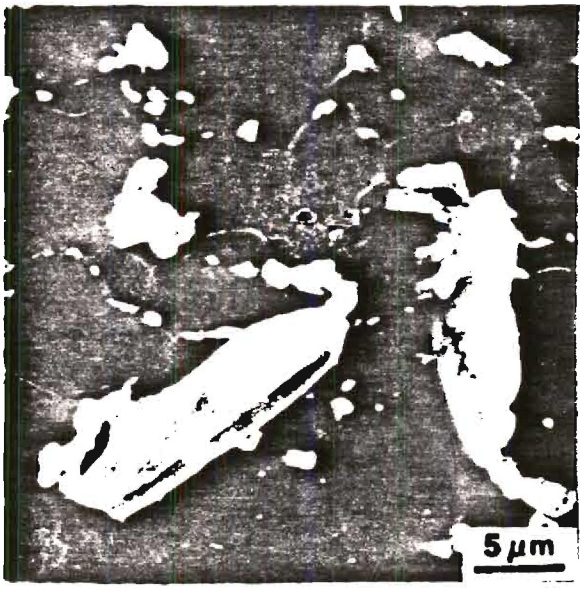

FIGURE 4. Scanning electron micrographs of bromine etched extruded alloy no. 1 SHT at 811K for 4.0 hrs.

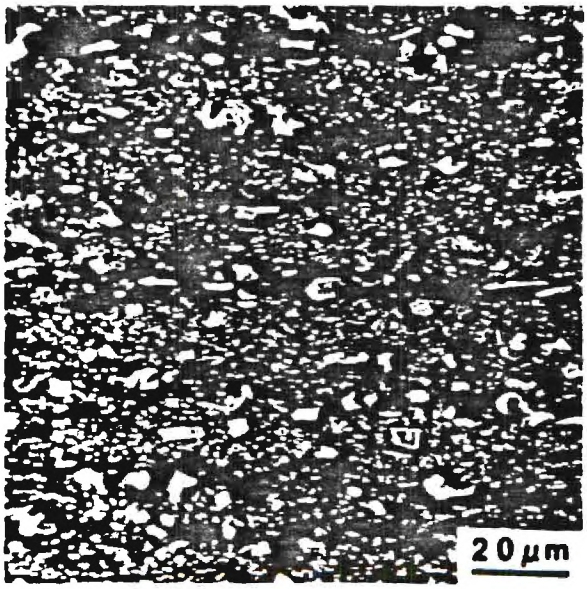

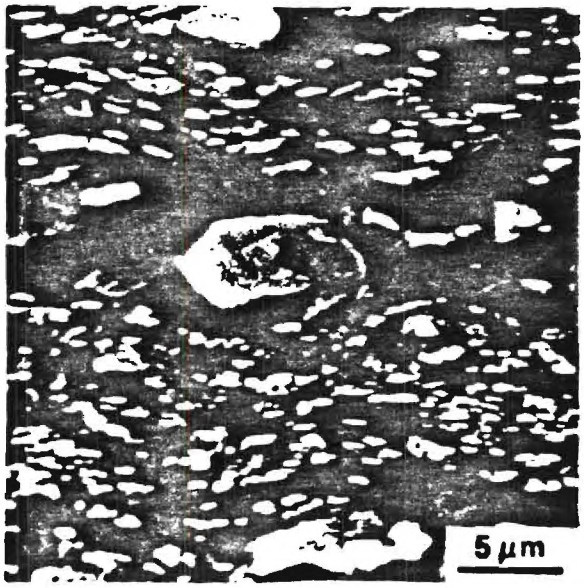

FIGURE 5. Scanning electron micrographs of bromine etched extruded alloy no. 2

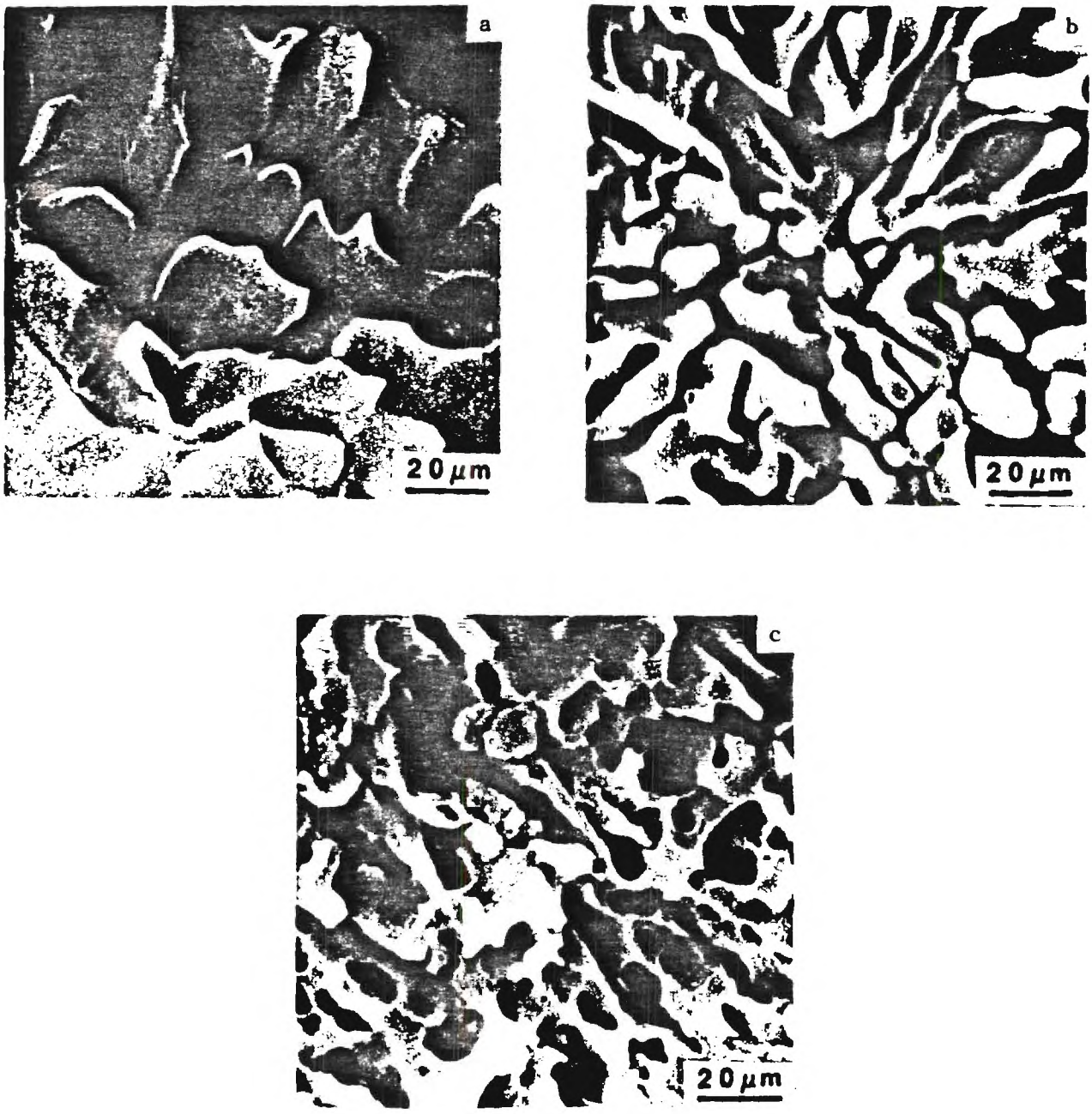

FIGURE 6. Scanning electron micrographs of sodium hydroxide etched RS powder particles of alloy no. 1. a) as-received condition, b) heat treated at 473K for 1.5 hrs, and c) heat treated at 655K for 5.0 hrs.

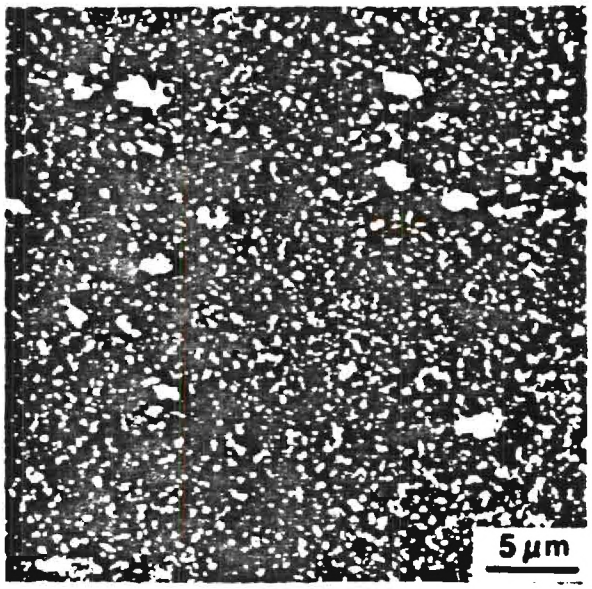

FIGURE 7. Scanning electron micrograph of bromine etched MA alloy Al-2.5Li-1.5Cu-1.0Mg.

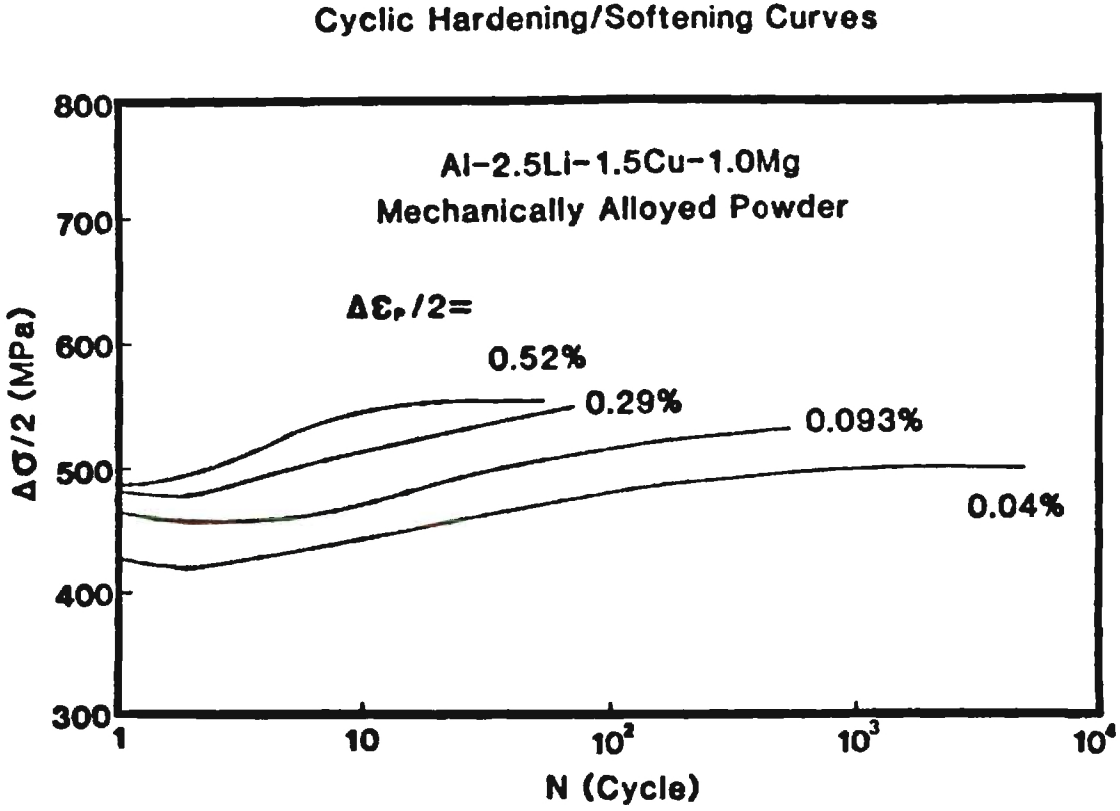
Cyclic Hardening/Softening Curves
Al-2.5Li-1.5Cu-1.0Mg
Mechanically Alloyed Powder
Δεp/2=
0.52%
0.29%
0.093%
0.04%
Δσ/2 (MPa)
800
700
600
500
400
300
1
10
10²
10³
10⁴
N (Cycle)

FIGURE 8.

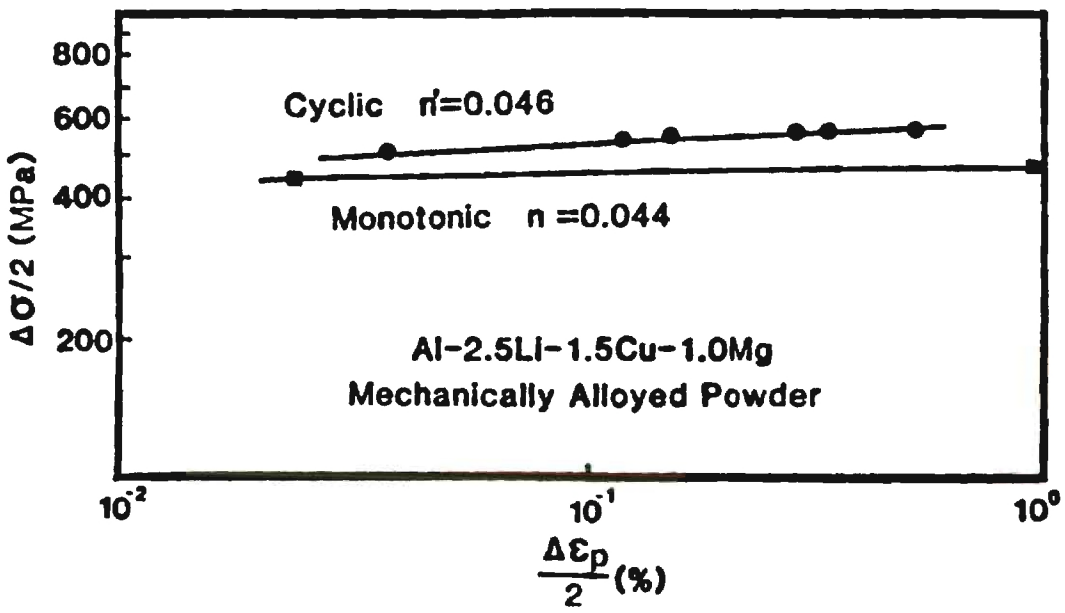

Monotonic And Cyclic Stress-Strain Curves

FIGURE 9.

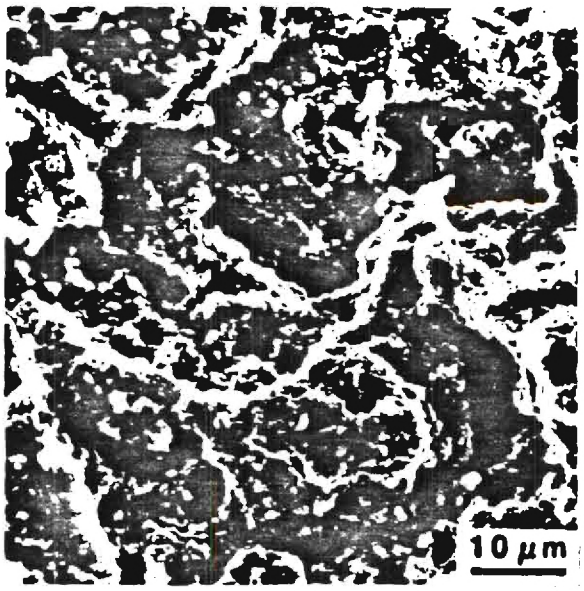

FIGURE 10. Scanning electron micrograph of LCF fracture surface.

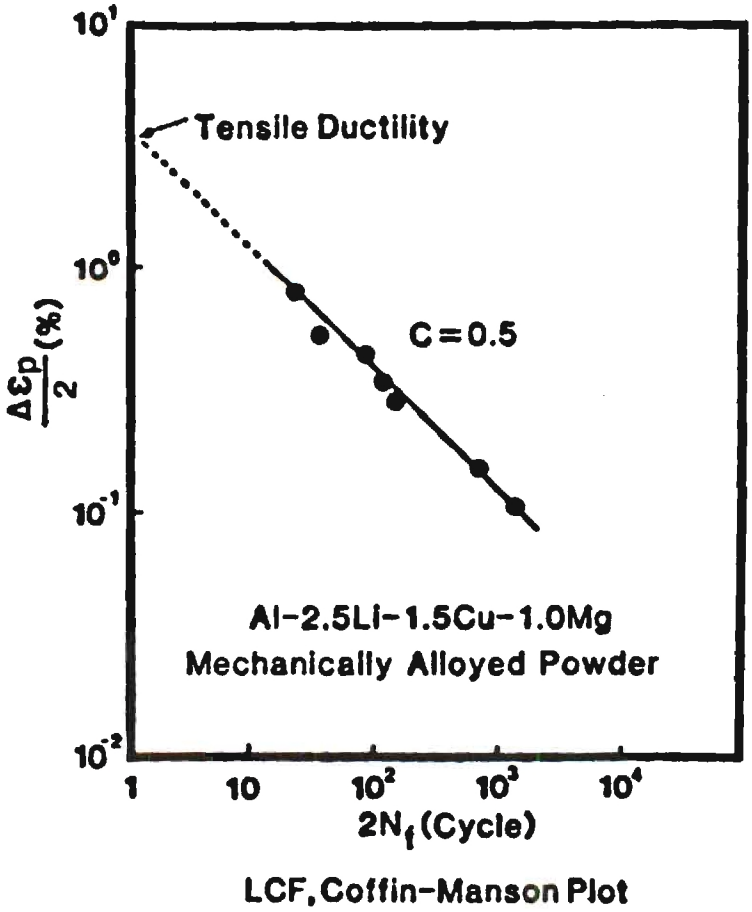

LCF, Coffin-Manson Plot

FIGURE 11.

Unclassified

SECURITY CLASSIFICATION OF THIS PAGE *(When Data Entered)*

REPORT DOCUMENTATION PAGE		READ INSTRUCTIONS BEFORE COMPLETING FORM
1. REPORT NUMBER	2. GOVT ACCESSION NO.	3. RECIPIENT'S CATALOG NUMBER
4. TITLE *(and Subtitle)* The Effects of Powder Metallurgical Processing and Intermediate Thermal Mechanical Treatment on the Fatigue Properties of High Strength Aluminum Alloys		5. TYPE OF REPORT & PERIOD COVERED Final Report 1 April 1980 - 31 March 1983 6. PERFORMING ORG. REPORT NUMBER
7. AUTHOR(s) Victor Kuo, H. Chang, and E.A. Starke, Jr.		8. CONTRACT OR GRANT NUMBER(s) DAAG29-80-C-100
9. PERFORMING ORGANIZATION NAME AND ADDRESS Fracture and Fatigue Research Laboratory		10. PROGRAM ELEMENT, PROJECT, TASK AREA & WORK UNIT NUMBERS
11. CONTROLLING OFFICE NAME AND ADDRESS U. S. Army Research Office Post Office Box 12211 Research Triangle Park, NC 27709		12. REPORT DATE 13. NUMBER OF PAGES 21
14. MONITORING AGENCY NAME & ADDRESS(if different from Controlling Office)		15. SECURITY CLASS. (of this report) Unclassified 15a. DECLASSIFICATION/DOWNGRADING SCHEDULE

16. DISTRIBUTION STATEMENT *(of this Report)*

Approved for public release; distribution unlimited.

17. DISTRIBUTION STATEMENT *(of the abstract entered in Block 20, if different from Report)*

18. SUPPLEMENTARY NOTES

The view, opinions, and/or findings contained in this report are those of the author(s) and should not be construed as an official Department of the Army position, policy, or decision, unless so designated by other documentation

19. KEY WORDS *(Continue on reverse side if necessary and identify by block number)*

powder metallurgy, aluminum alloys, fatigue, rapid solidification, thermomechanical processing

20. ABSTRACT *(Continue on reverse side if necessary and identify by block number)*

The application of advanced metallurgical processing techniques, e.g., intermediate thermomechanical treatment (ITMT) and powder metallurgy (P/M), has produced a recrystallized X7091 P/M alloy having fine grain and particle structures and weak texture with the best overall mechanical properties compared to those of ingot metallurgical and conventional P/M alloys. The dependence of mechanical properties on grain size and particle distribution has been demonstrated among these alloys. The

DD FORM 1 JAN 73 1473 EDITION OF 1 NOV 65 IS OBSOLETE

UNCLASSIFIED

SECURITY CLASSIFICATION OF THIS PAGE *(When Data Entered)*

20. continued

study of the effect of the last microstructural feature, crystallograph texture, is necessary for further property improvement through texture control.

A sharp retained deformation texture and a weak texture were introduced into two recrystallized P/M plates with similar grain size (about 15 μm) and fine particle distribution by ITMT's based on different recrystallization mechanisms. The difference in strength was mainly accounted for by the different values of Taylor factor with respect to the stress axis. Although the tensile fracture properties were similar, the fracture appearance varied with the degree of grain boundary misorientation. The texture effect on the stress-controlled fatigue appeared to be the modification in strength, even though the crack initiation mechanisms were different. The change in initiation mechanism was associated with the change in grain boundary misorientation and slip length. The variation in texture changed the crack morphology, deformation behavior and slip length during fatigue crack propagation. These factors led to a different degree of roughness-induced crack closure and slip reversibility at the crack tip, and resulted in the difference in crack growth rate. The improvements in strength and fatigue resistances have been obtained simply by introducing a sharp retained deformation texture into a recrystallized X7091 P/M plate.

The Effects of Powder Metallurgical Processing and Intermediate Thermal Mechanical Treatment on the Fatigue Properties of High Strength Aluminum Alloys

Final Report on Grant No.
DAAG29-80-C-100
April, 1983

by

Victor Kuo, H. Chang and E. A. Starke, Jr.
Fracture and Fatigue Research Laboratory
Georgia Institute of Technology
Atlanta, GA 30332

This Research was sponsored by the Army Research Office,
Research Triangle Park, NC under Grant Number DAAG29-80-C-100

Approved for Public Release, Distribution Unlimited

TABLE OF CONTENTS

LIST OF FIGURES

ABSTRACT

The application of advanced metallurgical processing techniques, e.g., intermediate thermomechanical treatment (ITMT) and powder metallurgy (P/M), has produced a recrystallized X7091 P/M alloy having fine grain and particle structures and weak texture with the best overall mechanical properties compared to those of ingot metallurgical and conventional P/M alloys. The dependence of mechanical properties on grain size and particle distribution has been demonstrated among these alloys. The study of the effect of the last microstructural feature, crystallographic texture, is necessary for further property improvement through texture control.

A sharp retained deformation texture and a weak texture were introduced into two recrystallized P/M plates with similar grain size (about 15 μm) and fine particle distribution by ITMT's based on different recrystallization mechanisms. The difference in strength was mainly accounted for by the different values of Taylor factor with respect to the stress axis. Although the tensile fracture properties were similar, the fracture appearance varied with the degree of grain boundary misorientation. The texture effect on the stress-controlled fatigue appeared to be the modification in strength, even though the crack initiation mechanisms were different. The change in initiation mechanism was associated with the change in grain boundary misorientation and slip length. The variation in texture changed the crack morphology, deformation behavior and slip length during fatigue crack propagation. These factors led to a different degree of roughness-induced crack closure and slip reversibility at the crack tip, and resulted in the difference in crack growth rate. The improvements in strength and fatigue resistances have been obtained simply by introducing a sharp retained deformation texture into a recrystallized X7091 P/M plate.

Introduction

Current studies[1-9] of high-strength Al-Zn-Mg-Cu (7XXX) alloys have focused on the development of powder metallurgical (P/M) alloys. The P/M X7091 alloy has shown improved monotonic, fatigue strength and resistance to stress corrosion cracking but inferior fracture toughness and resistance to fatigue crack propagation (FCP) when compared with ingot metallurgy (I/M) alloys.[1-4] Our initial studies involved microstructural modifications of X7091 using a variety of processing methods in order to obtain a better combination of mechanical properties.[1] With the exception of one product which had oxide-induced fracture, a reduction in grain size and a finer particle distribution increased the ductility and resistance to fatigue crack initiation (FCI) but decreased the resistance to FCP. An optimum microstructure, which consisted of small recrystallized grains, a fine particle distribution and a weak texture, was identified as having the best overall mechanical properties among the various microstructures studied. The details of this work were published recently in Metallurgical Transactions (Ref. 1), which is attached as Appendix A. In addition, we have conducted further studies on I/M X7091. That work is covered in the M.S. Thesis of H. Chang which is attached as Appendix B. Our most recent work, which will be covered in this final report, is directed towards further improvement in properties through texture control.

The non-uniform material flow during metal working and/or variations in heat-up rate during subsequent heat treatment usually result in differences in grain structure and texture throughout the thickness of most

high-strength aluminum products. Since particles greatly affect the recrystallization process, the presence of a uniform particle distribution may reduce the inhomogeneity of a recrystallized microstructure. In general, widely-spaced, coarse particles create strain concentrations at particle-matrix interfaces, while closely-spaced fine particles tend to lead to more uniform dislocation distribution after metal working. During subsequent annealing, the acceleration of recrystallization is usually associated with the former case, while retardation is associated with the latter case. The intermediate thermomechanical treatment (ITMT) of aluminum alloys is a practice of the former case. For a certain amount of reduction, the recrystallized grain size is closely related to the number density of coarse particles. The resulting texture depends on the predominant recrystallization mechanism.

The effect of texture on the strength of materials as predicted by the Taylor relationship has been generally accepted. Palmer et al[10] reported that the yield strength of an Al-Li P/M alloy decreased with the sharpness of the fiber texture, which decreased with increasing extrusion aspect ratio. This can be explained by the fact that most of the slip systems in the round-bar extrusion were unfavorably oriented for slip with respect to the tensile axis. When a material having planar slip characteristics, a fine particle distribution, and a random or weak texture is deformed, the grain boundaries can act as effective barriers to dislocation slip due to the high degree of grain boundary misorientation. The generation of multiple slip near grain boundaries to accommodate their incompatibility may result in more homogeneous deformation. The effectiveness of the grain boundary as a slip barrier decreases when the alignment of slip planes occurs in adjacent grains

of a sharply-textured material. In this case, the slip length is no longer limited to grain dimensions. The combined effects of the crystallographic orientation (with respect to stress axis) and slip length on deformation and fracture behavior may conclude the effect of texture on mechanical properties of a material.

Based on recrystallization theories and ITMT techniques, two annealing textures or texture intensities were introduced into a recrystallized P/M X7091 plate, while keeping other microstructural variables constant. Their effect on the monotonic and cyclic properties of this alloy will be described in this report.

Experimental

An extruded P/M X7091-T7E70 rectangular bar, having an unrecrystallized grain structure and a sharp extrusion texture, was commercially purchased from Alcoa, Alcoa Center, Pennsylvania. It was subjected to two ITMT's (Fig. 1) to produce two plates with similar recrystallized grain and particle structures but different textures. The Graff-Sargent etching solution was used to reveal the grain structure. Bromine etching was used to observe the particle distribution. Both plates showed fairly homogeneous grain and particle distributions throughout the thickness.

Crystallographic texture determinations were carried out using the x-ray reflection method. Fixed time increments were employed to collect intensity data over a polar orientation range from 0 to 70 degrees. A computer program was used to construct the pole figures in the form of equal value contours and to provide average, maximum and minimum

intensities. The higher-temperature rolled plate, designated as S, showed a higher degree of texture variation throughout the thickness than that of the lower-temperature rolled plate, designated as W.

In order to assess the effect of texture on the mechanical properties of an age-hardening alloy, it is convenient to choose an aging condition for which the effect of crystallographic orientation and grain boundary misorientation on deformation and fracture characteristics are most pronounced. In the peak-aged temper, dislocations shear the coherent and partially-coherent strengthening precipitates. Consequently, the deformation mode is predominantly planar and the effectiveness of the grain boundary as the slip barrier can be detected. Both plates were stretched 2.0 pct after being cold-water quenched from the recrystallization temperature and then aged to produce the peak strength, designated as T651.

All mechanical tests were performed on a closed loop servohydraulic machine. The flat specimens of 2.5 mm thick were selected from the thickness which possessed the highest contrast in texture between these two plates, with the stress axes parallel to the rolling direction. The specimens had a gauge width of 6.4 mm and a gauge length of 25.4 mm for the tensile tests. The tension-tension (R = 0.1), stress-controlled, high cycle fatigue (HCF) tests were conducted in a vacuum environment ($<2 \times 10^{-5}$ torr), with a frequency of 20 Hz, using specimens of 60 mm X 10 mm with a semi-round side notch (radius = 3 mm). Crack propagation tests were conducted in a vacuum environment, with R ratio of 0.1 and frequency of 30 Hz. The WOL-type, compact-tension specimens (H/W = 0.97) were used, and the crack propagated on a plane normal to the rolling

direction. A clip-on gauge was mounted at the end of the notch to measure the crack opening displacement periodically. A travelling microscope was equipped to measure the crack length, a, for every 0.3 mm after the crack advanced out of the plastic zone of previous loading within the ranges of plane strain condition and a/w's = 0.3-0.5. SEM was used to examine the fracture features.

RESULT AND DISCUSSION

Texture and Microstructure

The ITMT's used produced two differently textured, recrystallized plates with similar grain and particle structures. The pole figures from (111) reflections were utilized to interpret the textures through the plate thickness, and the x-ray diffracted intensities were also normalized with the aid of a randomly oriented powder sample. The texture varied from {110} <112> near the surface to a sharp {110}<001> at the center of the S plate. Actually, the {110}<001>is a compromise texture of {110}<112>, and the latter has been recognized as a retained deformation texture. The ratio of maximum intensity to average intensity ranged from 6 to 13 in this plate. The W plate had texture varying from a weak cube near the surface to a weak {110}<112> at the center, and the intensity ratio ranged from 2 to 4. Cube texture is a normal recrystallization texture for fcc materials. The difference in texture between these two plates may be associated with the difference in rolling temperatures, which produced different recrystallization mechanisms. The strain concentrations in deformation zones around the overaged particles after rolling

promoted particle-stimulated recrystallization during subsequent annealing, for the lower-temperature rolled W plate. The resulting weak texture was expected in accordance with the annealing texture formation theory developed by Humphreys[11] for a polycrystalline dispersion material. Dynamic recovery becomes more important with increasing rolling temperatures, therefore, the higher-temperature rolling produced a more homogeneously, deformed structure, which promoted continuous recrystallization and strain-induced grain boundary migration. This resulted in a sharp retained deformation texture for the S plate. The variation of texture through the thickness was mainly due to the non-uniform strain distribution during rolling and variations in heat-up rate during annealing from the surface to the center. Even though the variation was present, a very distinct texture difference existed between these two plates since they recrystallized by different mechanisms.

The samples for testing were selected from the center portion of the S plate with the intensity ratios ranging from 9 to 13, and from the portion slightly off the center of the W plate with the intensity ratio ranging from 2 to 4. The grain structure within these thicknesses had a grain diameter of a sphere with equivalent volume of about 15 μm and a grain shape parameter of about 0.32. Bromine etching showed a random distribution of particles with sizes less than 1 μm, which was similar to the particle structure of the as-received material. Therefore, most of the overaged coarse precipitates formed during extensive overaging were re-dissolved during the final anneal of the ITMT's. The heat treatments did not alter the fine distribution of dispersoids and constituent particles of the P/M alloy. Oxide stringers and clusters

had been broken up, although oxides were occasionally observed at the recrystallized grain boundaries during TEM studies. These two types of samples had similar grain and particle structures, but differed in the recrystallization texture by a factor of about 4.

Monotonic Properties

The monotonic properties obtained from the tensile testings are presented in TABLE I. The S plate showed an increase in yield strength (30 MPa) and elongation but a slightly lower value of reduction in area or ductility, compared to those of the W plate.

TABLE I. The monotonic properties of the differently-textured recrystallized plates at the T651 condition.

	Y.S. (MPa)	UTS (MPa)	Elongation (%)	$\ln\frac{A_o}{A}$(%)
S plate	558	587	12.9	29
W plate	528	571	10.8	33

Y.S. = proof stress, $\sigma_{0.2}$

$\ln\frac{A_o}{A}$ = ductility from reduction in area

The strengtn of an age hardening aluminum alloy is primarily associated witn precipitation strengthening although texture strengthening and grain boundary strengthening may also contribute. Since the aging condition and grain structure were similar in both plates, the difference in yield strength should be attributed to the difference in crystallographic orientation. According to the restricted slip theory for axisymmetric deformation, slip in the S plate had a lower-bound Taylor factor

value of about 2.45 compared to 2.24 for a randomly oriented polycrystalline material. This predicts a slightly higher strength for the S plate. The ratio of UTS/YS may indicate the degree of strain hardening during uniform deformation. The generation of more slip systems (multiple slip or homogeneous slip), due to the crystallographic orientation or to the grain boundary incompatibility, may be responsible for the higher degree of strain hardening of the W plate. The texture effect on strength and deformation may be associated with the crystallographic orientation dependence of slip activation and the promotion of homogeneous slip due to grain boundary misfit.

Both plates showed a shear-type, transgranular fracture. Fracture occurred by microvoid coalescence and the fracture surface of the S plate consisted of a relatively shallow dimple structure, while the secondary cracking along grain boundaries was an important fracture feature for the W plate. The uniform deformation throughout the gauge length yielded a slightly higher elongation of the S plate due to the similar orientation of the most grains. The shallow dimple structure may indicate that one slip system predominated up to fracture, consistent with the observed crystallographic texture. In contrast, the non-uniform distribution of strain may lead to early void nucleation at the grains which are favorably oriented for slip. This resulted in a slightly lower elongation and higher reduction in area for the W plate. However, the secondary cracking along these highly misoriented grain boundaries did not contribute a pronounced effect to the fracture properties of this plate.

The variation in recrystallization texture resulted in different

strength and other tensile properties. The effect of slip length was obscured, since the S plate did not show the characteristics of larger grains, e.g. low yield strength and low ductility.

Fatigue Crack Initiation

The S-N plots of the HCF tests are shown in Fig. 2a. There was a very slight degree of experimental scatter, compared to that of the other I/M 7XXX alloys, due to the homogeneous microstructures of these P/M alloys. The S plate showed a better FCI resistance in the long-life region. The FCI sites were located at the center of the specimen thickness. The cracks initiated at the slip bands, which covered several grains in the S plate, but were at both slip bands and grain boundaries in the W plate.

The strength of a material is usually the most significant factor in stress-controlled HCF. Fig. 2b illustrates the S-N curves normalized with the yield stresses in TABLE I. They became coincident with the modification of strength. Therefore, the texture effect on stress-controlled HCF was mainly due to its effect on the strength of these plates. However, the FCI mechanisms were different. The slip band initiation, which extended across about 4-8 grains, may have indicated that the slip distance may be several times the grain dimension of the S plate. Furthermore, this phenomenon may have been enhanced by the formation of persistent slip bands or strain localization which increased the stress concentration level at the intersection with the slightly-misoriented grain boundaries. Consequently, the resistance to FCI may be degraded since fatigue life normally decreases with increasing grain

size or slip length. On the other hand, the highly-misoriented grain boundaries promoted homogeneous deformation, which reduced the degree of strain localization, and eliminated the slip band cracking as the initiation mechanism. Such an improvement in FCI resistance has been reported for several aluminum alloys.[12,13] In the short-life region in Fig. 2b, the fatigue lives followed the trend described above. The difference became obscured with increasing fatigue life. This may be due to a very small amount of plastic strain being generated at the low stress amplitudes. Although the mechanisms for crack initiation were different, the effect of texture on the HCF lives was mainly accounted for by the difference in strength. Introduction of a weak texture may have improved the FCI resistance in the short-life region, but a sharp texture may have improved the resistance in the long-life region.

Fatigue Crack Propagation

Two sets of fatigue crack growth rate (FCGR) data were generated from a/w = 0.3 to 0.4 and 0.4 to 0.5, respectively. The stress intensity factor range (ΔK) was limited below 10 MPa $\sqrt{m}$ for the plane strain condition in this type of thin compact-tension specimen to be valid. Fig. 3 presents the FCGR's as a function of ΔK for the S and W plates. The FCGR's collected from a/w = 0.3 to 0.4 were about one order greater than those from a/w = 0.4 to 0.5. The crack in the S plate advanced slower than that in the W plate for the same a/w value range. The crack propagation was mostly transgranular and grew in a zig-zag fashion. The fracture features consisted of brittle facets at various angles with respect to the stress axis. The average facet size of the S fracture surface was several times that of the grain size, while the W fracture

surface had a facet size roughly corresponding to the grain size. The difference in FCGR's may be attributed to the difference in strength, deformation behavior, slip length and/or the degree of roughness-induced crack closure between these two differently-textured plates.

The accumulated damage model indicates that the crack advances when a maximum amount of plastic deformation has been accumulated at the crack tip. The strength of a material usually has less influence on the FCGR, compared to its cyclic ductility and cyclic strain hardening exponent. Fatigue crack closure may also have an effect on the FCGR. The crack closure stress intensity factor, K_c, derived from the crack opening displacement, was plotted against the FCGR's of these two plates in Fig. 4 for different a/w values. The K_c's were larger for propagation over a/w values between 0.4 and 0.5 than for a/w values between 0.3 and 0.4. The longer crack appears to have experienced a higher degree of crack closure. There was significant scatter in the K_c data as shown in Fig. 4. However, the S cracks showed slightly larger values of K_c than those of the W cracks. Since most of the grains had a similar crystallographic orientation, the crack front did not change propagation direction dramatically as it crossed the grain boundaries, until other crack planes became preferred mechanically. This phenomenon yielded a fracture surface with large facets, which had experienced a higher degree of roughness-induced crack closure compared to the fine-faceted W fracture surface. Consequently, the rougher fracture surface slowed down the fatigue crack growth in the sharply-textured S plate.

In order to understand the effects of deformation behavior and slip length on FCGR's of these two plates, ΔK_{eff}, substrating K_c from

K_{max}, is used to represent the ΔK at which the crack actually propagated. Figure 5 shows the FCGR's as a function of ΔK_{eff}. The S plate has slower FCGR's than those of the W plate, despite the wide scatter bands due to the scattered K_c values. According to the accumulated damage model, the less the plastic deformation is accumulated at the crack tip, the slower the fatigue crack grows. With the consideration of crystallographic texture, under a certain amount of normal stress, the plastic strain response of the S plate was smaller due to its larger Taylor factor value with respect to the stress axis. Since the grain boundary did not act as an effective barrier to dislocation slip in a sharply-textured material, the slip length was probably larger than the grain dimension of the S plate. The large facets on the fracture surface were partially a result of this phenomenon. The studies of grain size dependence of FCGR have indicated that the dislocation slip was more reversible on a long slip band during fatigue.[14] Therefore, the less plastic strain response and the more reversible slip reduced the accumulation rate of plastic deformation at the crack tip for the S plate. In contrast, a higher accumulation rate may have occurred in the W plate, because of its homogeneous deformation, generation of geometrically-necessary dislocations at grain boundaries and less reversible slip on a short slip band. Consequently, the different deformation behavior resulted in the difference in FCGR's between S and W plates.

The effect of recrystallization texture on the FCGR's in these two materials, included its effect on crack morphology, slip length and deformation behavior. The amount of plastic strain response during each loading cycle was determined by the crystallographic orientation.

The increase in texture sharpness increased the fracture surface roughness and slip length, but reduced the slip homogeneity. Roughness-induced crack closure and the accumulated damage model suggest that all these factors reduced the FCGR of the sharply-textured S plate. Further improvement on the resistance to FCP of the 7XXX alloys may be accomplished by introducing a sharp retained deformation texture in a recrystallized P/M alloy.

CONCLUSIONS

1. Two recrystallized plates having similar grain and particle structures, but different textures (or texture intensities) by a factor of 4, were produced by ITMT's based on different recrystallization mechanisms.
2. The variation in strength was related to the difference in the Taylor factor value with respect to the stress axis. The sharply-textured plate showed a greater yield strength (about 30 MPa).
3. The tensile fracture appearance varied with the degree of grain boundary misorientation. Although the two plates had similar fracture properties, secondary cracking along grain boundaries was prevalent in the weakly-textured plate.
4. The texture effect on the stress-controlled HCF appeared to be the modification in strength, although the FCI mechanism may also change. The cracks were initiated at slip bands, which covered several grains in the sharply-textured plate, and at both slip bands and grain boundaries in the weakly-textured plate. The change

in FCI mechanism was associated with the change in grain boundary misorientation and slip length.

5. The variation in texture changed the crack morphology, deformation behavior and slip length during FCP. The coarse fracture features enhanced the roughness-induced crack closure. Also, a longer slip distance and greater slip reversibility reduced the accumulation rate of plastic strain at the crack tip. All these factors led to the higher FCP resistance of the sharply-textured plate.
6. The further improvement in overall mechanical properties, which included a higher strength, longer HCF lives and greater FCP resistance, was obtained by introducing a sharp retained deformation texture into a recrystallized X7091 P/M plate.

SCIENTIFIC PERSONNEL

Dr. Edgar A. Starke, Jr., Co-Principal Investigator

Dr. Saghana B. Chakrabortty, Co-Principal Investigator

Victor W.C. Kuo, Graduate Student
M.S. Georgia Institute of Technology
PhD Georgia Institute of Technology expected August, 1983

Hao Chang, Graduate Student
M.S. Georgia Institute of Technology, June, 1983

Publications and Technical Reports

1. Victor W.C. Kuo and E.A. Starke, Jr., "The Effects of ITMT's and P/M Processing on the Microstructure and Mechanical Properties of the X7091 Alloy" in Michael J. Koczak and Gregory J. Hildeman, eds., High Strength Powder Metallurgy Aluminum Alloys, The Metallurgical Society of AIME, Warrendale, PA, 1982 pp. 41-63.

2. Victor W.C. Kuo and E.A. Starke, Jr., "The Effect of ITMT's and P/M Processing on the Microstructure and Mechanical Properties of the X7091 Alloy," Met. Trans. A. 14A (1983) pp. 435-447.

3. Hao Chang, "The Effect of an Intermediate Thermomechanical Treatment on the Fatigue Properties of I/M X7091 Aluminum Alloy," M.S. Thesis, Georgia Institute of Technology, Atlanta, GA, June, 1983.

4. Victor W.C. Kuo, "The Effects of Powder Metallurgical Processing and Intermediate Thermal Mechanical Treatment on the Fatigue Properties of High Strength Aluminum Alloys, X7091," M.S. Thesis, Georgia Institute of Technology, Atlanta, GA, August, 1981.

References

1. Victor W.C. Kuo and E.A. Starke, Jr., Metall. Trans. A, 1983, vol. 14A, p. 435.

2. J.P. Lyle, Jr. and W.S. Cebulak, Met. Eng. Quart., 1974, vol. 14, no. 1, p. 52.

3. J.P. Lyle, Jr. and W.S. Cebulak, Metall. Trans. A, 1975, vol. 6A, p. 685.

4. W.S. Cebulak, E.W. Johnson, and H. Markus, Met. Eng. Quart., 1976, vol. 16, no. 4, p. 37.

5. S. Hirose and M.E. Fine, High-Strength Powder Metallurgy Aluminum Alloys, M.J. Koczak and G.J. Hildeman, eds., TMS-AIME, Warrendale, PA, 1983, p. 19.

6. M. Rafalin, A. Lawley, and M.J. Koczak, High-Strength Powder Metallurgy Aluminum Alloys, M.J. Koczak and G.J. Hildeman, eds., TMS-AIME, Warrendale, PA, 1983, p. 63.

7. S. L. Langenbeck, High-Strength Powder Metallurgy Aluminum Alloys, M.J. Koczak and G.J. Hildeman, eds., TMS-AIME, Warrendale, PA, 1983, p. 87.

8. Y.W. Kim and L.R. Bidwell, High-Strength Powder Metallurgy Aluminum Alloys, M.J. Koczak and G.J. Hildeman, eds., TMS-AIME, Warrendale, PA, 1983, p. 107.

9. J.R. Pickens, J.R. Gordon, and L. Christodoulou, High-Strength Powder Metallurgy Aluminum Alloys, M.J. Koczak and G.J. Hildeman, eds., TMS-AIME, Warrendale, PA, 1983, p. 177.

10. I.G. Palmer, R.E. Lewis, and D.D. Crooks, Aluminum-Lithium Alloys, T.H. Sanders and E.A. Starke, Jr., eds., TMS-AIME, Warrendale, PA, 1981, p. 241.

11. F.J. Humphreys, Acta Metall., 1977, vol. 25, p. 1323.

12. R.E. Sanders, Jr. and E.A. Starke, Jr., Thermomechanical Processing of Aluminum Alloys, J.G. Morris, ed., TMS-AIME, Warrendale, PA, 1978, p. 50.

13. R.E. Sanders, Jr. and E.A. Starke, Jr., Metall. Trans. A, 1978, vol. 9A, p. 50.

14. J. Lindigkeit, G. Terlinde, A. Gysler, and G. LUtjering, Acta Metall., 1979, vol. 27, p. 1717.

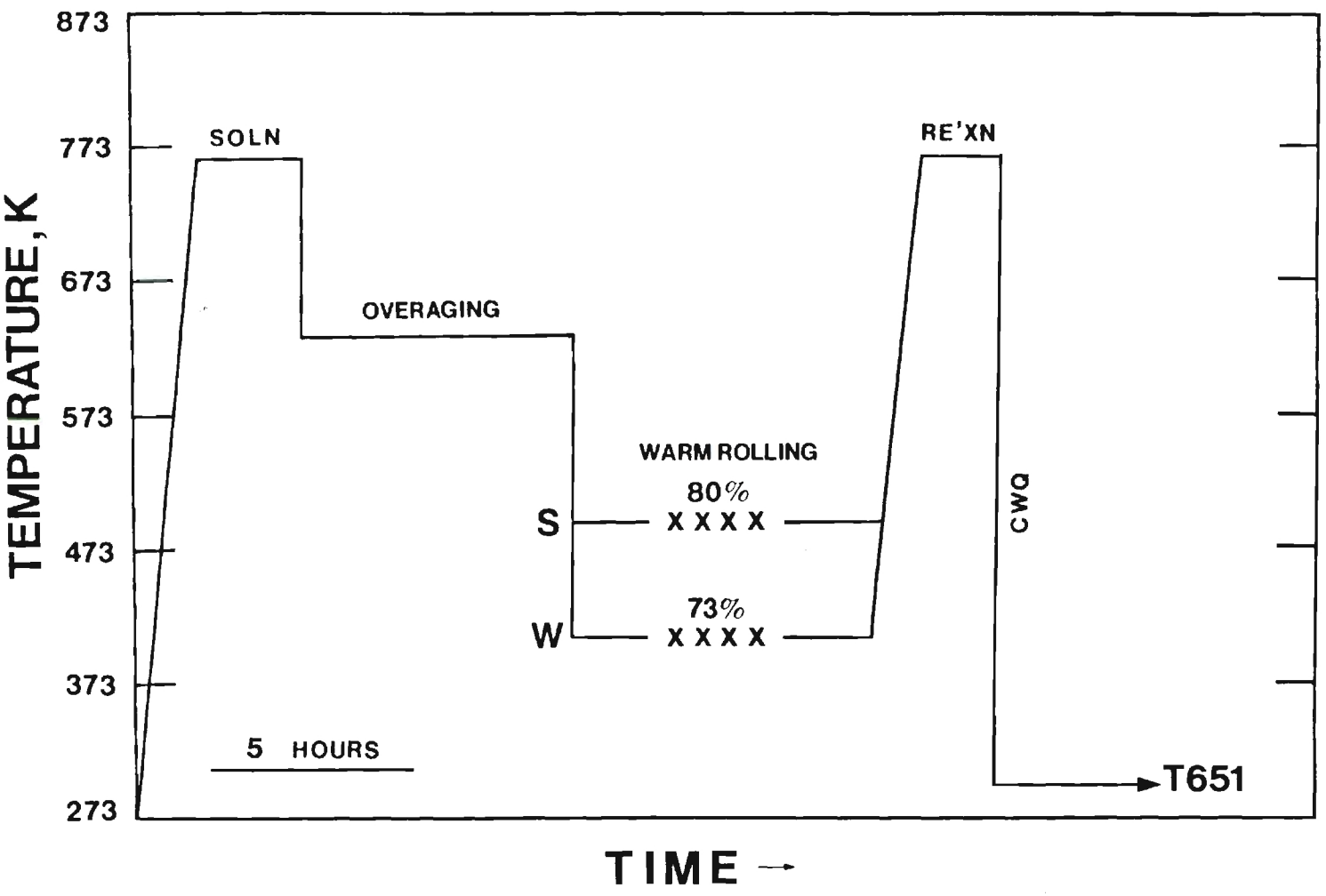

Figure 1. The ITMT schedules used to produce the S and W plates.

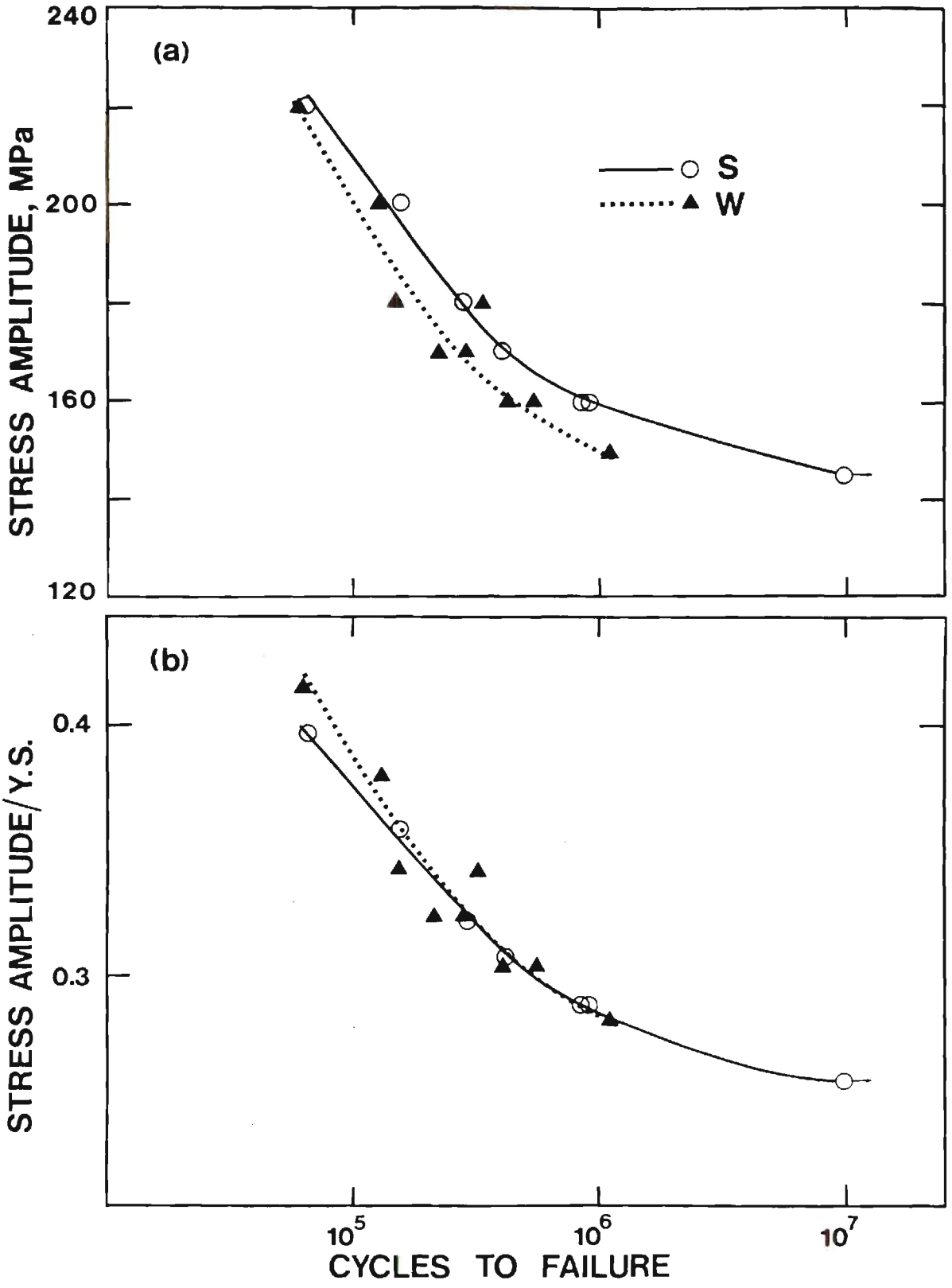

Figure 2. The HCF S-N curves showing (a) stress lives, and (b) normalized stress lives of the S and W plates.

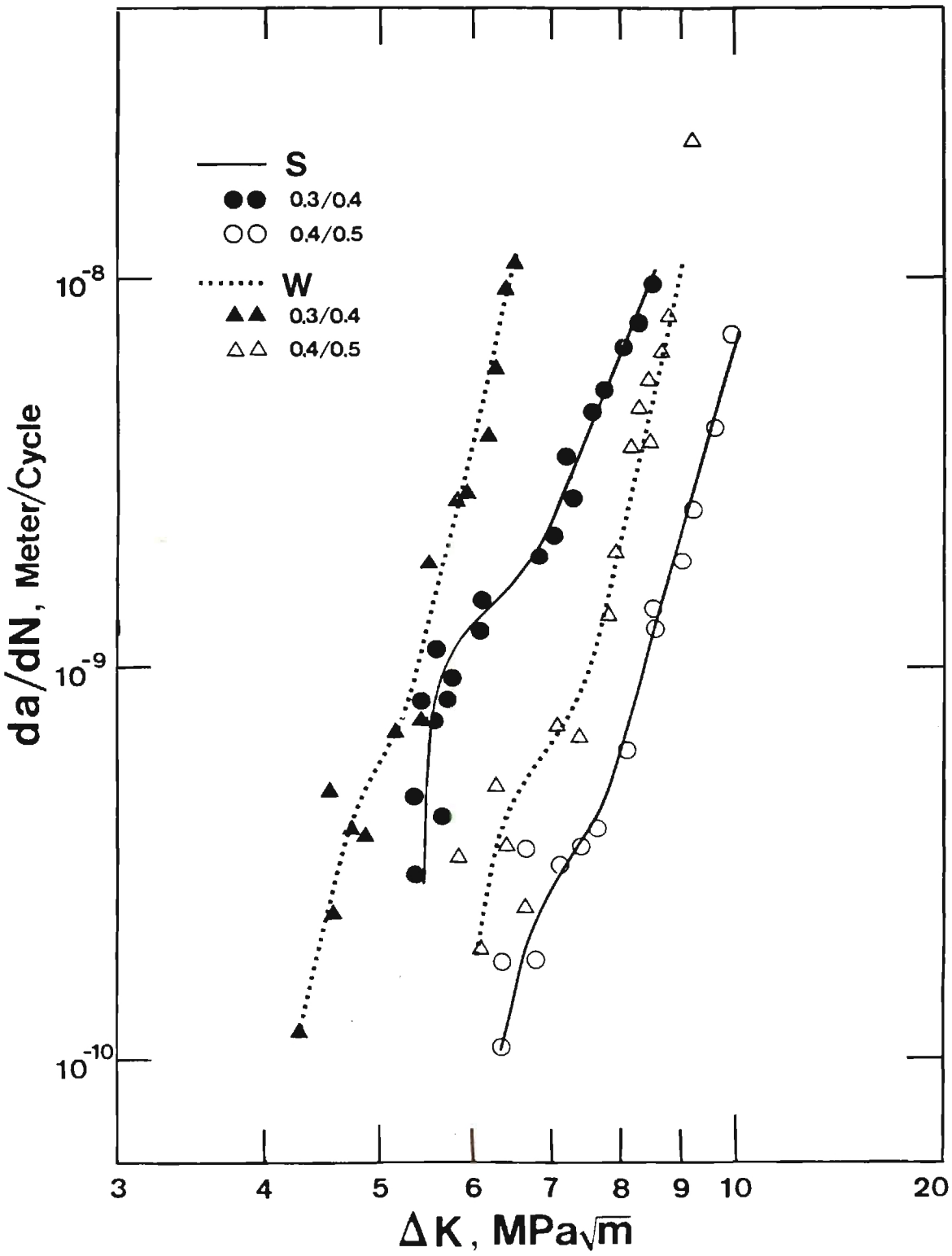

Figure 3. The FCGR's as a function of ΔK for a/w values of 0.3-0.4 and 0.4-0.5, for the S and W plates.

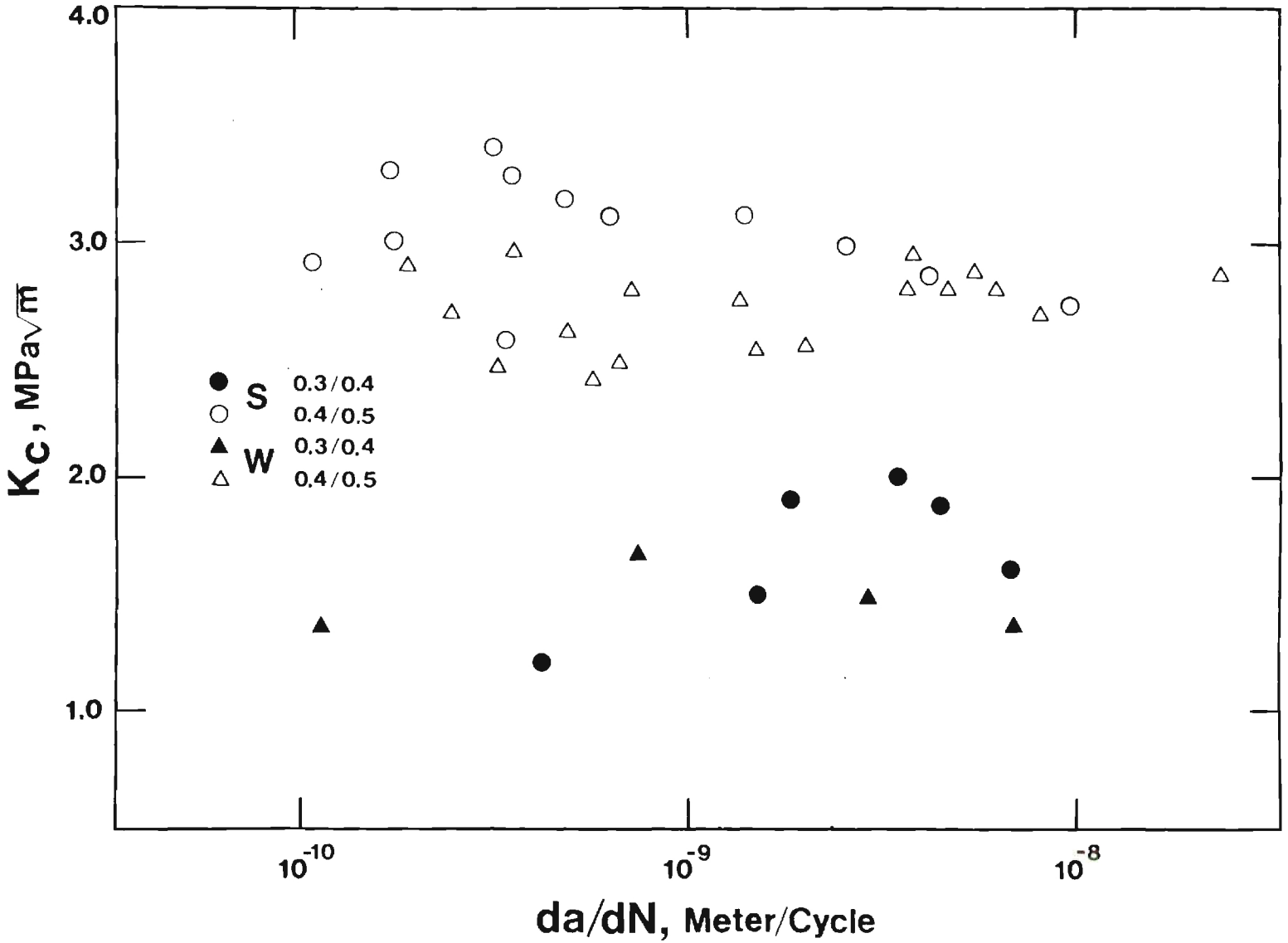

Figure 4. The crack closure stress intensities, K_c's, as a function of FCGR and a/w values for the S and W plates.

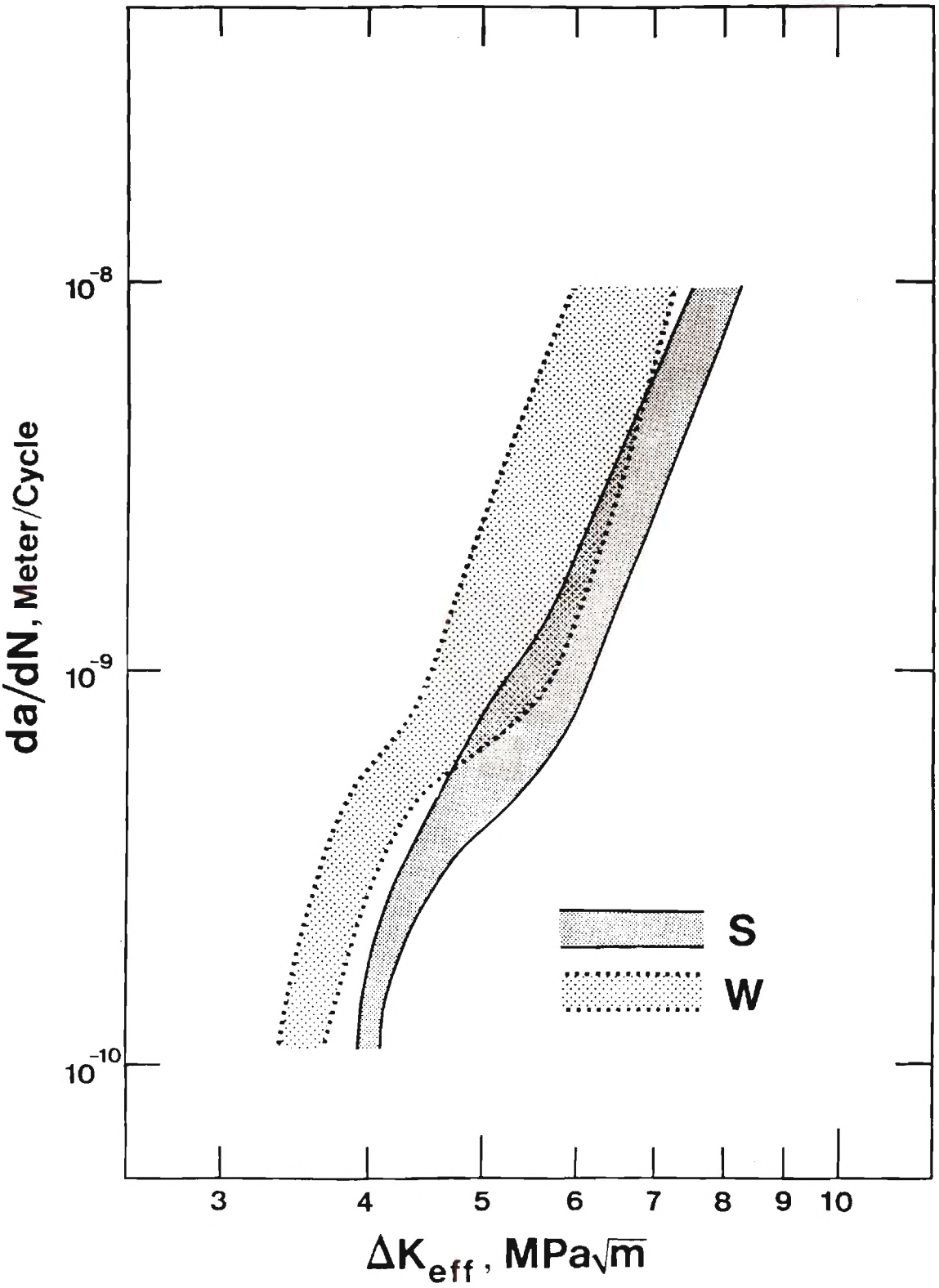

Figure 5. The FCGR's as a function of effective stress intensity, K_{eff}, for the S and W plates.